8-1-2013

EFFECT OF SUBSTRATE COMPOSITION ON MICROBIAL DIVERSITY AND EFFICIENCY OF in situ PILOT-SCALE PASSIVE SULFATE-REDUCING BIOREACTORS TREATING ACID MINE DRAINAGE

Charles Wayne Pugh
Southern Illinois University Carbondale, cpugh13@gmail.com

EFFECT OF SUBSTRATE COMPOSITION ON MICROBIAL DIVERSITY AND EFFICIENCY OF *in situ* PILOT-SCALE PASSIVE SULFATE-REDUCING BIOREACTORS TREATING ACID MINE DRAINAGE

by

Charles Wayne Pugh

B.S., Southern Illinois University, 2010

A Thesis
Submitted in Partial Fulfillment of the Requirements for the
Master of Science Degree

Department of Molecular Biology, Microbiology, and Biochemistry
in the Graduate School
Southern Illinois University Carbondale
August 2013

THESIS APPROVAL

EFFECT OF SUBSTRATE COMPOSITION ON MICROBIAL DIVERSITY AND EFFICIENCY OF *in situ* PILOT-SCALE PASSIVE SULFATE-REDUCING BIOREACTORS TREATING ACID MINE DRAINAGE

By

Charles W. Pugh

A Thesis Submitted in Partial

Fulfillment of the Requirements

for the Degree of

Master of Science

in the field of Molecular Biology, Microbiology, and Biochemistry

Approved by:

Dr. Kelly Bender, Chair

Dr. Antje Rusch

Dr. Derek Fisher

Graduate School
Southern Illinois University Carbondale
June 27th, 2013

AN ABSTRACT OF THE THESIS OF

Charles Pugh, for the Masters degree in Microbiology, presented on June 27th, 2013 at Southern Illinois University Carbondale.

TITLE: EFFECT OF SUBSTRATE COMPOSITION ON MICROBIAL DIVERSITY AND EFFICIENCY OF *in situ* PILOT-SCALE PASSIVE SULFATE-REDUCING BIOREACTORS TREATING ACID MINE DRAINAGE

MAJOR PROFESSOR: Dr. Kelly Bender

Acid mine drainage (AMD) is an environmental problem of a global scale. Passive remediation strategies utilizing the metabolism of sulfate-reducing bacteria have emerged as promising options for the mitigation of impacted AMD sites. In order to test the effect of varying complex and simple carbon sources on AMD remediation efficiency, pilot-scale bioreactors were constructed and exposed to AMD *in situ* over a ten-month period. Geochemical analyses suggested that the efficiency of AMD remediation depended more on the seasonal weather patterns of Southern Illinois, USA than the substrate composition of each bioreactor. Enrichment cultures targeting sulfate-reducing organisms yielded several isolates most closely related to members of the genera *Desulfovibrio* and *Clostridium*. Microbial community analysis was performed using fluorescent *in situ* hybridization, 16S rRNA gene targeted pyrosequencing, and quantitative polymerase chain reaction (qPCR). Results suggested that the depth from which samples were taken as well as the substrate composition impacted the microbial communities within each bioreactor. Over the course of the experiment the community changed from one similar to that of a bovine rumen to one more adapted to the acidic nature and high metal content of AMD. Community abundance based on 16S rRNA gene and *dsrB* gene copy number suggested an overall decrease in the bacterial population over the course of the study.

TABLE OF CONTENTS

CHAPTER PAGE

ABSTRACT i

TABLE OF CONTENTS ii

LIST OF TABLES iii

LIST OF FIGURES iv

CHAPTERS

CHAPTER 1 – Introduction 1

CHAPTER 2 – Materials and Methods 12

CHAPTER 3 – Results 26

CHAPTER 4 – Discussion 59

REFERENCES 74

APPENDICES

Appendix A Flourescent in situ hybridization raw data 82

Appendix B Flourescent in situ hybridization statistics 85

VITA 86

LIST OF TABLES

TABLE PAGE

Pilot-scale bioreactor substrate composition 13

Modified Postgate's Medium C components 16

FISH probes used in current study 18

Statistical tests of variance 55

FISH Counts for Bioreactor 1 Ports 82

FISH Counts for Bioreactor 2 Lower Ports 82

FISH Counts for Bioreactor 2 Upper Ports 82

FISH Counts for Bioreactor 3 Lower Ports 83

FISH Counts for Bioreactor 3 Upper Ports 83

FISH Counts for Bioreactor 4 Lower Ports 83

FISH Counts for Bioreactor 4 Upper Ports 84

FISH Counts for Bioreactor 5 Lower Ports 84

FISH Counts for Bioreactor 5 Upper Ports 84

FISH Counts for Bioreactor 6 Lower Ports 84

FISH Counts for Bioreactor 6 Upper Ports 84

FISH Statistical Analysis 85

LIST OF FIGURES

FIGURE PAGE

Proposed Geomicrobiological model of AMD Sediment ……...4

Bioreactor at Tab-Simco Mine site ……8

Workflow for QIIME 16S Pyrosequencing Analysis 24

Bioreactor Outflow and Regional Temperature 26

Bioreactor Effluent pH Values 27

Bioreactor Influent pH Values 28

Bioreactor ORP Values 29

Bioreactor Percentage of Sulfate Removed 30

Phylogenetic Tree of *Desulfovibrio* Related Isolates 31

Phylogenetic Tree of *Clostridium* Related Isolates 32

Relative Abundances Determined by FISH 33

Relative Bacterial Class Abundance from August 2012 35

Rarefaction Analyses for August 2012 Sample Data 37

Diversity Measures for August 2012 Samples 38

Genus Level Heatmap for August 2012 Samples ……39

Principal Coordinate Analysis of August 2012 Samples ..…….....40

3D PCoA Scatter Plot of August 2012 Samples 42

August 2012 UPGMA Hierarchical Cluster Tree 43

Relative Bacterial Class Abundance from May 2013 45

Rarefaction Analyses for May 2013 Sample Data 47

Diversity Measures for May 2013 Samples 48

Genus Level Heatmap for May 2013 Samples 50

Principal Coordinate Analysis (PCoA) of May 2013 Samples 52

3D PCoA Scatter Plot of May 2013 Samples ……...53

May 2013 UPGMA Hierarchical Cluster Tree 54

16S rRNA Gene qPCR 56

dsrB Gene qPCR 58

CHAPTER 1

INTRODUCTION

Acid Mine Drainage Generation

Acid mine drainage (AMD) is an environmentally impactful consequence of mining activity characterized by low pH, high sulfate, and high concentrations of heavy metals and sulfate (Colmer, 1947). AMD is formed through a series of biological and chemical reactions that result in the oxidation and dissolution of pyrite (FeS_2) (Singer, 1970). Mining activities increase the surface area of exposed pyrite dramatically and thus instigate a situation in which the natural attenuation capabilities of the surrounding environment can be overwhelmed (Schippers, 2010; Singer, 1970). While the detailed mechanisms are still a matter of debate, in general, AMD is a result of pyrite (and other sulfidic compounds, i.e. marcosite and magnetite) exposure to oxygenated water according to the following reaction (Baker, 2002; Singer, 1970):

$$FeS_{2(s)} + 3.5\ O_2 + H_2O \rightarrow Fe^{2+} + 2\ SO_4^{2-} + 2\ H^+ \qquad [1]$$

The resultant ferrous iron (Fe^{2+}) is then oxidized to ferric iron (Fe^{3+}) at low pH (pH<4) according to the reaction (Sánchez, 2005; Singer, 1970):

$$14\ Fe^{2+} + 3.5\ O_2 + 14\ H^+ \rightarrow 14\ Fe^{3+} + 7\ H_2O \qquad [2]$$

The ferric iron generated from reaction 2 is an even stronger oxidant of pyrite in lower pH environments than oxygenated water. Thus, the ferric iron generated in the initial reaction

re-oxidizes pyrite, generating more acidity and ferrous iron in a self-perpetuating cycle of reduction and oxidation. This process is illustrated in the following reaction (Sánchez, 2005; Johnson, 2012; Singer, 1970):

$$FeS_{2(s)} + 14\ Fe^{3+} + 8\ H_2O \rightarrow 15\ Fe^{2+} + 2\ SO_4^{2-} + 16\ H^+ \qquad [3]$$

Due to the higher rate of pyrite oxidation and the increased proton generation by ferric iron when compared to that of the O_2 catalyzed reaction, the oxidation of ferrous iron is considered the rate-limiting step of acid generation from pyrite oxidation (Singer, 1970). While the abiotic oxidation of ferrous iron is relatively slow, the presence and activity of iron-oxidizing bacteria (FeOB) can increase the ferrous iron oxidation rate by factors greater than 10^6 (Edwards, 1998; Johnson, 2003). Although the actual rate of biotic pyrite dissolution is still poorly understood, a seminal study on the topic conducted by the Banfield group suggests that up to 75% of AMD produced is the direct result of microbial activity (Edwards, 1998). In particular, the activity of two commonly identified FeOB within AMD communities, (*Acidithiobacillus ferrooxidans* and *Leptospirillum ferrooxidans*) are suspected to facilitate ferrous iron oxidation in both planktonic and biofilm communities, e.g. indirectly and through direct contact (Denef, 2010; Dopson, 2012). Due to the small energetic yield and autotrophic metabolisms of most FeOB, approximately 55 g of ferrous iron must be oxidized for each dry gram of biomass generated (Haferburg, 2007). This presents a situation in which the microbial community continually generates a large amount of oxidized iron species, leading to an increased rate of acid and sulfate generation.

Metal complexes present in the mined ores are mobilized in the low pH water generated from pyrite oxidation, hydrolyzed, and precipitated as hydroxides when mixed in cleaner waters, producing acidity and further exacerbating the drop in pH and impact of AMD on the environment (Schipper, 2010; Singer, 1970). Due to the much greater solubility of cationic metals (i.e. aluminum and the previously discussed iron species) in low pH waters, unusually high metal concentrations are also indicative of AMD and contribute to its toxicity (Druschel, 2004). The U.S. Forest Service estimates that up to 50,000 mines are currently generating AMD (Jennings, 2008). AMD generated from such sites are suspected to endure indefinitely if untreated. AMD impacted water sources result in massive reduction in fish and invertebrate populations as well as loss of vegetation that rely on such water sources (Jennings, 2008).

Biogeochemical Model of AMD Sediments

Bacteria play a major role in expediting and perpetuating the formation of AMD. Source points of AMD as well as other extremely acidic environments are commonly lacking for direct sunlight and are relatively oligotrophic (Johnson, 1998). As such, the vast majority of metabolic activity in such environments is chemolithoautotrophic and relies on the oxidation and reduction of iron and sulfur. The work of several groups at various sites around the world have allowed insights into the types of geochemical interactions required to sustain the microbial ecosystem in such a unique environment. Figure 1 shows an adaptation of a sediment/water column model proposed by Sánchez-Andrea *et. al* in 2011 (Sánchez-Andrea, 2011).

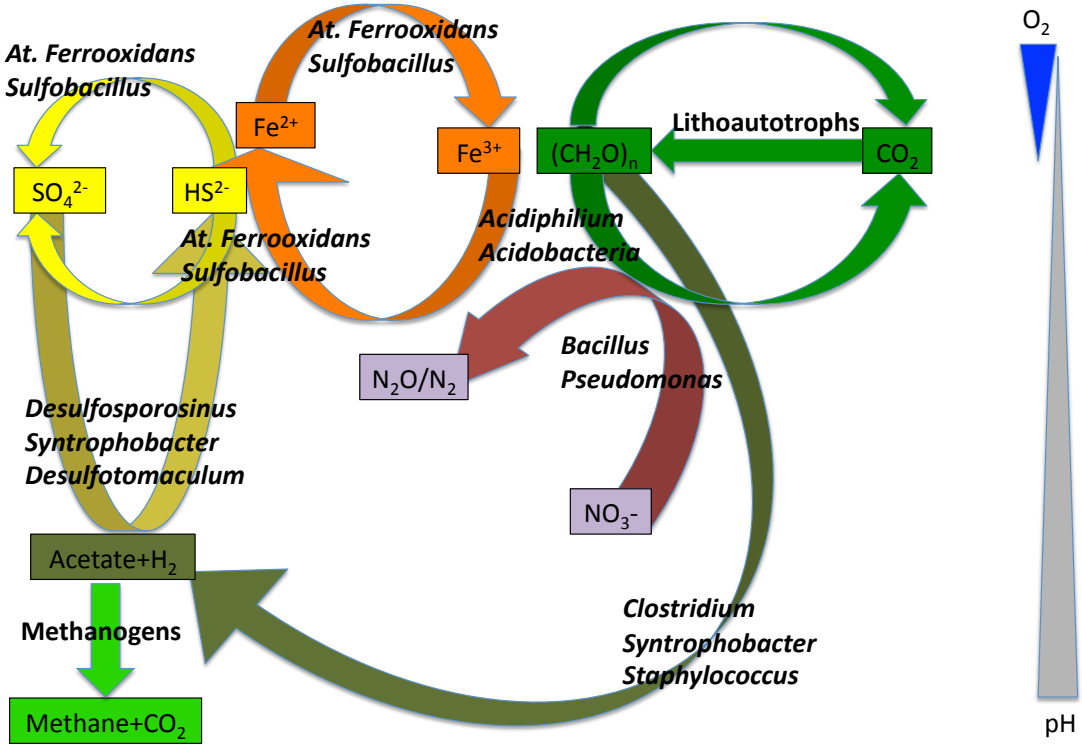

Figure 1. Proposed Geomicrobiological model of AMD Sediment Model of microbially-mediated interactions between the Sulfur (yellow), Iron (orange), Carbon (green), and Nitrogen (red) cycles. Bars represent oxygen concentration and pH, respectively. Information for figure from Baker *et. al*, 2003, Sánchez-Andrea *et. al*, 2011, and Burns *et. al*, 2011.

This model is based on data from the Rìo Tinto AMD site. Iron, in both its oxidized and reduced form plays a key role in the metabolic cycle of AMD sediments. Lithoautotrophic sulfur- and iron-oxidizing organisms contribute to the small pool of available organic compounds with the excretion of carbon compounds not assimilated into biomass (Baker, 2003). Organisms such as *Acidithiobacillus ferrooxidans* are capable of oxidizing ferrous iron to ferric iron both anaerobically and aerobically (Sánchez-Andrea, 2011; Lu, 2010). The ferric iron, which can reach high concentrations in low pH sediments and water, can then serve as an electron acceptor

for the oxidation of organic molecules by heterotrophic organisms like *Acidiphilium* and *Acidobacteria* species (Sánchez-Andrea, 2011; Baker, 2003). Ferric iron reduction can also be coupled to the anaerobic oxidation of organic compounds as well as sulfides to sulfate by *At. ferrooxidans* and *Sulfobacillus* species (Sánchez-Andrea, 2012; Sánchez-Andrea, 2011, Baker, 2003).

Clostridium and other organotrophic species break down organic carbon compounds through a fermentative pathway that results in a mix of intermediates, including acetate and hydrogen. The resultant small carbon compounds can then be utilized by sulfate-reducing bacteria (SRB) like *Desulfotomaculum* and *Desulfosporosinus* species for the reduction of sulfate (Sánchez-Andrea, 2011). It is also likely that methanogens are present in the community and that they compete with SRB for small organic compounds (Sánchez-Andrea, 2011). Nitrate reduction may be linked to the oxidation of organic compounds by species of *Bacillus* and *Pseudomonas,* although relatively little is known about the nitrogen cycle in AMD generating environments (Sánchez-Andrea, 2011).

AMD Remediation

The low pH and elevated heavy metal and sulfate concentrations of AMD make it an environmental concern of paramount importance in areas replete with abandoned coal mines such as the American Midwest. Over 15,000 kilometers of surface water are currently impacted by acid mine drainage in the United States alone (Baldwin, 2009). Billions of dollars are spent each year on the treatment and management of AMD worldwide. Legislation requiring the

remediation of contaminated sites has created a need for low-cost and low-maintenance options for mitigating AMD damage to the environment.

Due to the toxicity, persistence and prevalence of AMD contamination it is essential to develop methods to remediate AMD. Both biotic as well as abiotic remediation options have been employed at numerous AMD sites. As reviewed by Johnson and Hallberg, abiotic methods involve addition of chemicals designed to raise water pH, coat AMD generating rocks, and inhibit the biotic processes responsible for AMD generation (Johnson, 2005). While several biological strategies for AMD remediation have been employed, passive sulfate-reducing bioreactors (PSRBs) have become a popular choice due to their relative inexpensiveness and minimal maintenance requirements (Macias, 2012).

PSRBs rely on the metabolism of heterotrophic sulfate-reducing bacteria (SRB) to reduce sulfate present in AMD waters (Song, 2012; Sánchez-Andrea, 2012). The reduction of sulfate to hydrogen sulfide (H_2S) requires eight electrons and several enzymes. Because of the relative stability of sulfate it must first be activated with ATP, a reaction catalyzed by the enzyme ATP sulfurylase (Madigan, 2009). The resultant molecule, adenosine phosphosulfate (APS) is then reduced to sulfite by the enzyme APS reductase (Madigan, 2009). Sulfide is then further reduced to hydrogen sulfide by the enzyme dissimilatory sulfite reductase (Dsr) (Madigan, 2009). The *dsrAB* genes are conserved amongst SRB and share approximately 60% sequence homology across all species in which they have been found (Dahl, 1993). This conservation and homology has made the *dsr* genes a useful tool in the phylogenetic arsenal of SRB study (Wagner, 1998). Similar to 16S rRNA genes, primers targeting the *dsr* genes can be used to examine and characterize the sulfate-reducing community present in ecological systems (Baker, 2003).

During the remediation process, sulfate reduction aids in metal precipitation and pH neutralization (Kijjanapanich, 2012; Johnson, 2005). Biotic sulfate reduction is generally expressed according to the following equation (Postgate, 1984):

$$2\ CH_2O + SO_4^{2-} \rightarrow 2\ HCO_3^- + H_2S \quad [4]$$

Where CH_2O represents a number of simple organic carbon sources with low molecular weight (e.g. lactate, acetate, ethanol) (Nancucheo, 2011; Norlund, 2009). The resultant bicarbonate (HCO_3^-) serves a dual-purpose in raising the pH of the drainage and promoting the formation of metal carbonates (Song, 2012; Norlund, 2009). The various sulfur compounds produced also facilitate metal precipitation by forming metal sulfides as follows (Zagury, 2006; Johnson. 2005):

$$H_2S + Me^+ \rightarrow MS + 2\ H^+ \quad [5]$$

In which Me^+ represents a cationic metal. While it has recently been suggested that sulfate reduction can occur in low pH environments; most SRB are active in circum-neutral pH (pH 5-8) environments (Oren, 2010).

PSRBs function by funneling AMD downward through an organic matrix which functions in removing dissolved oxygen and promoting sulfate reduction (Bekmezci, 2011). In most cases AMD is channeled through ditches or tunnels lined with limestone or treated with an alkalinity producing substance in order to raise the pH of the AMD to a value more suitable for sulfate reduction (Gadd, 2010). AMD is then held in an acid pond above the bioreactor, as seen

in **Figure 2**. The AMD then passes through the established organic matrix and is retained for a period (dependent on surface area and matrix composition) to allow time for sulfate reduction to occur (Church, 2007). Metals are then precipitated out of the system via formation of insoluble sulfides, hydroxides, and carbonates (Bekmezci, 2011; Macias, 2012). Bioreactor effluent is then filtered through mesh-filters to collect sulfides. Alternatively, the treated effluent is allowed to flow through constructed "wetlands" with a circumneutral pH where further oxidative processes occur and the precipitated metals are collected downstream prior to reintroduction into a natural body of water (Baldwin, 2009).

Figure 2. Bioreactor at Tab-Simco Mine site October 2012 Photo of the acid pond covering the constructed bioreactor at the Tab-Simco site outside of Carbondale, IL, USA.

The most integral function of a PSRB is providing an optimal physiochemical environment for SRB and other organisms that facilitate sulfate reduction and metal precipitation (Lovely, 1993). The organic matrix layer provides electrons for reductive processes, including sulfate reduction, via the degradation of the complex organic matter contained within the matrix (Hiibel, 2008; Johnson, 2005). Organic substrate choice is critical to the success of PSRB function and longevity (Song, 2012). For example, the commonly used substrate mixture known as "mushroom compost" has been shown to be a poor source of available organic carbon for most SRB and thus requires supplementation with other substrates for effective long-term functioning (Neculita, 2011; Neculita, 2008). Several laboratory studies have reported that combining cellulosic (wood chips, sawdust, etc.) and mixed organic substrates (manure, compost, brewing wastes) resulted in improved AMD treatment in long-term experiments (Neculita, 2007, Zagury, 2006). To further demonstrate the benefit of mixed substrate bioreactors, Neculita *et al.* reported that after 70 days mixed organic waste substrates harbored over 10^4 more SRB than cellulosic wastes despite the release of up to 44% more total organic carbon (TOC) from cellulosic substrates (Neculita, 2011). While not explicitly proposed by the authors, this data suggests that while mixed organic wastes may be more effective at stimulating SRB in the short term, the sequential breakdown of cellulosic wastes may provide a reservoir of simple organic substrates for SRB utilization after the mixed organic wastes have been utilized.

Despite the mounting evidence in favor of mixed-substrate compost mixtures, the literature is essentially devoid of attempts to assess the relative effectiveness of variable organic layer constituents *in situ*. This is especially true for microbial studies; there is a paucity of data on the microbial communities present in PSRBs remediating AMD. Although there is no question that other factors (i.e. clogging, flow-rate flux, substrate run-off) influence the

effectiveness and longevity of PSRBs, determining the optimal organic matrix layer composition may contribute to the long-term solution of AMD remediation.

Previous Research

Previous work performed on the Tab-Simco mine site, an abandoned mine in Giant City State Park, Carbondale, Illinois has been published (Burns, 2012). Geochemical data collected 10 months post bioreactor construction suggested that the system was successfully mitigating AMD pH (pH increased from 3.09 to 6.65), iron (95.9% removal) and sulfate (67.4%) concentrations. Biological sulfate reduction was indicated by an increase in $\delta^{34}S$ of 2.6% in bioreactor outflow waters. 16S rRNA and *dsrAB* gene clone libraries were used to analyze the microbial community present in pre- and post-bioreactor samples. Pre-treated waters were dominated by sequences similar to iron-oxidizing *Betaproteobacteria*. Post-treatment samples were dominated by sequences similar to sulfur-oxidizing members of the *Epsilonproteobacteria* along with *Bacteroidetes* and *Firmicutes*, specifically sequences similar to carbon degrading organisms. Analysis of the *dsrAB* gene clone library suggested limited SRB community diversity in both pre- and post-remediation samples. While the data presented in the article suggested a relatively well functioning bioreactor system, continued measurements showed a drastic decrease in pH mitigation and contaminant removal over time (Pugh, 2012). This decrease in bioreactor efficiency led to the proposal of the current study.

Research Aims

After the constructed remediation system at the Tab Simco site ceased functioning properly, pilot-scale bioreactors were constructed on-site. Varying ratios of simple and complex carbon sources were utilized is each bioreactor. Microbial community analyses and geochemical measures were used to determine the shift in the microbial community over time. This provides a chance to examine the effect of different PSRB substrate concentrations on the efficiency of AMD remediation utilizing PSRBs under actual AMD and environmental conditions. At the conclusion of the full study, optimal carbon source composition ratios can be determined for the construction of full scale PSRBs.

CHAPTER 2

MATERIALS AND METHODS

Study Site

The study site for this work was the abandoned Tab-Simco coal mine. The site, located Southeast of Carbondale, IL, USA, consists of approximately 121,406 m^2 of underground mine works that have been discharging AMD through several series of man-made seeps that eventually flow into the nearby Sycamore Creek (Smith, 2002). It was reported as one of the most highly contaminated AMD sites in the mid-continent region and designated as a target for remediation in 1996 (Behum, 2011; Smith, 2002). A 3,000 m^2 PSRB consisting of a compost layer of 53% woodchips, 27% straw mulch, 11% seasoned compost, and 9% limestone was constructed in October of 2007 (Behum 2011; Burns, 2012). The water chemistry and flow-rate of the pre- and post-treatment AMD from the site has been monitored since the construction date (Behum, 2011; Lefticariu, Unpublished Data).

Bioreactor Construction

At the Tab-Simco site, six 0.21 m^3 polyethylene barrel pilot-scale bioreactors were constructed on the embankment through which AMD is funneled from the main seep to the acid pond holding area. A weir system was constructed to dam the main seep stream and channel the AMD into polyvinyl chloride (PVC) piping where it was then distributed into each bioreactor. Sampling ports were inserted at 0.3 m intervals with PVC screw caps and butyl stoppers to allow for sampling from various depths within the bioreactors. Port 1 in each bioreactor was located

above the substrate layer, ports 2 and 3 were located within the substrate layer, and the fourth port (labeled as Outflow) was located in the limestone layer. The distribution system was designed so that each of the six bioreactors experienced a continuous flow rate proportional to the flow rate of the actual on-site bioreactor (2.9 L/day). Each bioreactor contained mixtures of simple and organic substrates with a total volume of 176 liters as shown in **Table 1**.

Table 1 Pilot-scale bioreactor substrate composition.

Substrate	Reactor 1	Reactor 2	Reactor 3	Reactor 4	Reactor 5	Reactor 6
	0	(50:50)*	(70:30)	(30:70)	(90:10)	(10:90)
	(L)	(L)	(L)	(L)	(L)	(L)
Whey	0	8.8	8.8	8.8	8.8	8.8
Manure	0	17.6	17.6	17.6	17.6	17.6
Leaf Compost	0	28.6	39.6	13.2	55.1	5.2
Spent Brewing Grains	0	8.8	13.2	13.2	8.8	2.6
Grass Clippings	0	28.6	39.6	13.2	55.1	5.3
Maple Wood Chips	0	33	19.8	46.2	6.6	59.5
Maple Saw Dust	0	33	19.8	46.2	6.6	59.5
Limestone	17.6	17.6	17.6	17.6	17.6	17.6

*(X:Y) represents ratios of complex to simple substrates as defined in the text. All units in liters.

Sampling and Geochemical Analyses

Sampling

Water and sediment samples were collected from the pilot-scale bioreactors one week (August, 2012) after they were exposed to the on-site AMD and ten months post-exposure (May, 2013) for microbial community analyses. Members of the Lefticariu lab also took water samples bi-monthly for geochemical analyses. Water and small particles of substrate were extracted in duplicate from each port with a 50 ml syringe and 22-gauge needle. Samples for pyrosequencing were evacuated into 50 ml conical tubes and placed on ice and stored at 4°C upon return to the lab until further processing. Samples for fluorescent *in situ* hybridization (FISH) were extracted and evacuated in the same manner. A 15 ml sample from each port set (Port 1 and 2; Port 3 and Outflow) was immediately preserved with 15 ml of 4% paraformaldehyde solution and placed on ice before being stored at 4°C for 5 h. After incubation, 5 and 10 ml volumes of each sample were filtered onto 0.2 μm pore-size, 47 mm GTTP Isopore polycarbonate membrane filters (Millipore), rinsed with distilled H_2O, air-dried and stored at -20˚C (Fuchs, 2010).

Geochemical Analyses

Evan Walters of the Lefticariu Laboratory in the Department of Geology (SIUC) performed the geochemical analyses of the pilot-scale reactor water samples. The pH and oxidation-reduction potential of the outflow from each port was measured *in situ* with a HQ40D pH/conductivity/DO Meter (Hach). Sulfate and other anions were measured using ICS-2000 (Dionex) ion chromatography with KOH eluent and an IonPack® AS18-HC (Dionex) column (Behum, 2011).

Sulfate-Reducing Enrichments

Traditional culture techniques were utilized in order to enrich for and isolate organisms capable of reducing sulfate within the bioreactors. For SRB isolation, a medium based on Postgate's Medium C (**Table 2**) was utilized (Postgate, 1984). Sulfate (40 mM) was provided as the terminal electron acceptor along with varying electron donors (acetate, pyruvate, ethanol, methanol) in 10 mM, 20 mM and 30 mM concentrations. Enrichment pH was adjusted to values representing the expected possible pH range (3.5-8.0) found within the bioreactor substrate layers. The medium was inoculated with water/sediment samples from Port 2 and Port 3 of each bioreactor containing a substrate mixture (Reactors 2-6). Enrichments were grown in an anaerobic chamber (Coy) at 30˚C for 1 week. Serial dilutions of 10^{-1} to 10^{-5} were carried out on enrichments showing visible signs of possible sulfate reduction, (color change, black precipitate formation, turbidity) plated on solid agar medium, (Modified Medium C plus 15% agar) and checked for colony formation. Resultant colonies were repeatedly transferred to fresh Medium C, plated on solid Medium C, and monitored with light microscopy for evidence of uniform cell morphology and colony formation until deemed a pure culture.

Table 2 Modified Postgate's Medium C components.

Component	Final Conc.	Volume (per liter)
0.5 M $NaSO_4$	40 mM	80.0 ml
1 M $MgCl_2$	8 mM	8.0 ml
4 M NH_4Cl	20 mM	5.0 ml
1 M K_2HPO_4-NaH_2PO_4	2 mM	2.0 ml
1 M $CaCl_2$	0.6 mM	0.6 ml
1X Trace Minerals[1]	½ X	12.5 ml
2 M Tris-HCl, pH 7.4	30 mM	15.0 ml
Yeast Extract	0.25 g/L	0.25 g
Adjust pH with NaOH		
Added after autoclave		
10X Thauer's Vitamins[2]	1 X	1.0 ml
For plates		
Agar	15 g/L	12.5 g

[1]Trace minerals contained the following per liter of degassed ddH_2O: 12.8 g Nitrilotriacetic acid; 1.0 g $FeCl_2 \cdot 4H_2O$; 0.5 g $MnCl_2 \cdot 4H_2O$; 0.3 g $CoCl_2 \cdot 6H_2O$; 0.2 g $ZnCl_2$; 0.05 g $Na_2MoO_4 \cdot 4H_2O$; 0.02 g H_3BO_3; 0.1 g $NiSO_4 \cdot 6H_2O$; 0.002 g $CuCl_2 \cdot 2H_2O$; 0.006 g Na_2SeO_3; 0.008 g $Na_2WO_4 \cdot 2H_2O$. pH was adjusted to 6.5 and filter sterilized through a 0.2 µm filter.

[2]10X Thauer's vitamins consisted of the following per liter of degassed ddH_2O: 0.02 g d-Biotin; 0.02 g Folic Acid; 0.1 g Pyridoxine Hydrochloride; 0.05 g Thiamine Hydrochloride; 0.05 g Riboflavin; 0.05 Nicotinic Acid; 0.05 g Pantothenic Acid; 0.05 g p-Aminobenzoic Acid; 0.05 g Thioctic Acid; 2.0 g Choline Chloride; 0.01 g Vitamin B12. pH was adjusted to 7.0 and filter sterilized through a 0.2 µm filter.

Fluorescent *in situ* Hybridization

FISH targeting rRNA was used to assess the bacterial community of each barrel on a class level. Each probe was 5'-labeled with either a green or red fluorescent tag, Atto488 or Cy3, respectively. Probes, as shown in **Table 3**, were either synthesized by Biomers.net (Ulm, Germany) or provided by Dr. Antje Rusch (SIUC). Filters were then cut into $1/16^{th}$ sections and hybridized with 2 µl of probe (50 ng/µl) in 20 µl of hybridization buffer (18% 5M NaCl, 2% 1M

Tris/HCl pH 7.5, X% formamide depending on probe (Table 3), 0.1% sodium dodecyl sulfate (SDS), and Y% H_2O depending on probe). Each filter section was covered in 20 µl of the probe/buffer solution and placed in a 50 ml conical tube with blotting paper soaked in ~2 ml hybridization buffer. The filter/probe mixture was then incubated for 2 hours in a 46˚C hybridization oven (Boekel Bambino). After incubation the hybridized filters were washed in 50 ml of a washing buffer (X ml 5M NaCl, depending on formamide concentration in the hybridization buffer, 1 ml 1 M Tris/ HCl, 500µl 0.5M EDTA, H_2O to 50 ml, 50 µl 10% SDS) in a 48˚C water bath for 15 min. Filters were then washed in distilled water for several seconds and air-dried. Dried filters were then counterstained with 20 µl of 4',6-diamidino-2-phenylindole (DAPI) at 1 mg/ml concentration for 6 min. Counterstained filters were washed in distilled water and 80% ethanol sequentially before being air-dried and mounted with *SlowFade*® Gold Antifade Reagent (Molecular Probes, Inc.). A coverslip was placed over the top of the filters before they were viewed at 1000X total magnification using epifluorescent microscopy (Leica EL6000). DAPI- and probe-stained cells were counted in 24 fields of view.

For statistical analysis of FISH data, the F-test and T-test were used. The F-test compares population variances while the T-test compares population means. These tests were used to compare abundances from each bioreactor to each other. The cell counts for each sample were tested for significant difference from all other samples and against the non-probe count. Any relative abundance that was not statistically significant from the non-probe count was counted as zero.

Table 3 FISH probes used in current study.

Probe[a]	Target Organism[b]	Sequence	Formamide %	Reference
BET42a	*Betaproroteobacteria*	5' GCC TTC CCA CTT CGT TT 3' **c1** 5' GCC TTC CCA CAT CGT TT 3'	35	Manz et al. 1992
ALF968	*Alphaproteobacteria* (79%)	5'- GGT AAG GTT CTG CGC GTT -3'	20	Neef et al. 1997
DELTA495a	*Deltaproteobacteria* (73%)	5'- AGT TAG CCG GTG CTT CCT -3' **c1** 5'- AGT TAG CCG GTG CTT CTT -3'	35	Loy et al. 2002
Acido189	*Acidobacteria*	5'- CTG AGA TGG TTC ACT TCC -3'	20	Meisinger et al. 2007
EUB338	Most Bacteria (90%)	5'- GCT GCC TCC CGT AGG AGT -3'	35	Amann et al. 1990
Non338	None	5'- ACT CCT ACG GGA GGC AGC -3'	35	Wallner et al. 1993

[a]Probes for each listed target group were found using the online database probeBase (Loy, 2007). [b]Percentages indicate coverage of indicated target group. Probes BET42a and Acido189 have disputed or unpublished coverage.

DNA Extraction

Bioreactor Sample DNA Extraction

Samples for pyrosequencing were processed within 48 h of returning to the lab. Duplicate samples from each port were centrifuged at 5,000 X *g* for 15 min to settle large particles. The samples were then vacuum filtered through 0.2 µm sterile analytical test filters. The test filters

were cut using a sterile scalpel and split for duplicate DNA extractions. The solid fractions at the bottom of each tube were removed aseptically, separated into halves for duplicate extraction, and placed in a Lysing Matrix E tube. Total DNA was then isolated, in duplicate, directly from the filters and particle fractions using the FastDNA® SPIN Kit for Soil (MP Biomedicals). Briefly, 978 µl of Sodium Phosphate Buffer and 122 µl of MT Buffer were added to each filled Lysing Matrix E tube and were placed in a Biospec Mini Bead Beater (Bio Spec Products) on the highest setting for 40 s. Tubes were then centrifuged at 14,000 x *g* for 15 min. The supernatant from each tube was then transferred to a clean 2 ml tube and 250 µl of Protein Precipitation Solution was added. Tubes were inverted by hand 10 times before centrifugation at 14,000 x *g* for 5 min. Supernatant from each tube was transferred to a 15 ml conical tube and 1 ml of Binding Matrix Suspension was added. Tubes were inverted by hand for 2 minutes before 500 µl was removed. 600 µl of each suspension was added to a separate SPIN™ Filter and centrifuged at 14, 000 x *g* for 1 min. Filters were then washed with 500 µl of SEWS-M each and centrifuged at 14,000 x *g* for 3 min. DNA was eluted from the filter with 100 µl of DES each and stored at -20˚C. Concentration and purity of the resulting DNA was determined using Nanodrop spectrophotometry (Thermo Scientific) before being stored at -80˚C.

Enrichment Culture Genomic DNA Extractions

In order to determine the identity of isolates from enrichment cultures using the 16S rRNA gene, the Wizard® Genomic DNA Purification Kit (Promega) was used. Briefly, 3 ml of culture was spun at 5,000 x *g* for 5 min and the supernatant was removed through decanting and blotting on paper towels. The cell pellets were gently resuspended in 600 µl of Nuclei Lysis Solution. The cell suspensions were then incubated at 80˚C for 5 min. 3 µl of RNase Solution

was added to the suspensions before 30 min incubation at 37˚C. 200 µl of Protein Precipitation Solution was added and the mixtures were vortexed for 20 s prior to 5 min incubation on ice. The mixture was then centrifuged at 14,000 x *g* for 3 min. The resulting supernatant was then transferred to a clean microcentrifuge tube containing 600 µl of room temperature 100% isopropanol and inverted by hand. The tubes, containing precipitated DNA strands, were then centrifuged at 14,000 x *g* for 2 min. The supernatant was then removed, 600 µl of room temperature 70% ethanol was added, and the tubes were gently inverted several times. The ethanol was then aspirated and the tubes were air dried for 15 min. 30 µl of DNA Rehydration Solution was then added and the DNA pellets were stored overnight at 4˚C. Concentration and purity of the resulting DNA was determined using Nanodrop spectrophotometry (Thermo Scientific) prior to storage at -20˚C.

Sequencing and Analysis

Partial 16S rRNA Analysis

Polymerase Chain Reaction (PCR) was performed on each isolated DNA using a master mix consisting of 19 µl GoTaq buffer containing MgCl (Promega), 0.2 mM of each dNTP, 10 pmol of each primer, 1 Unit GoTaq® Polymerase (Promega), and 1 µl of DNA from SRB enrichment culture DNA extractions in a total volume of 50 µl. The primers used to target the bacterial 16S rDNA were Bac8F (5'-AGA GTT TGA TCC TGG CTC AG-3') and Univ529R (5'-ACC GCG GCK GCT GGC-3'). The 16S rRNA gene PCR consisted of a 94°C denaturating step for 2 min followed by 30 cycles consisting of 94°C for 30 s, 55°C for 30 s, and 72°C for 60 s followed by a final 5-min extension at 72°C. Resulting PCR products were analyzed by gel

electrophoresis and amplicons of the correct size (~500 bp) were excised and purified with the GeneJET Gel Extraction Kit (Thermo Scientific). Briefly, amplicons were cut out of 0.7% agarose gels with a clean razor blade and placed into a 1.5 ml microcentrifuge tube and weighed. Binding buffer was added at 1:1 (weight:volume). The gel mixtures were then incubated at 50˚C for 10 min with mixing every 2 min to ensure the gel was completely dissolved. The resultant solubilized gel solution was then added to a GeneJET purification column and centrifuged for 1 min at 14,000 x *g*. An additional 100 µl of Binding Buffer was added to the column with another round of centrifugation. The column was then washed with 700 µl of Washing Buffer and centrifuged. The DNA was then eluted from the column using 30 µl of Elution Buffer.

Resultant DNAs were then cloned into the pJET 1.2 Cloning Vector (Thermo Scientific) using the Sticky-End Cloning Protocol. Briefly, a blunting reaction (10 µl 2X Reaction Buffer, 3 µl gel-purified PCR product, 4 µl nuclease-free water, and 1 µl DNA Blunting Enzyme) was set up on ice and incubated at 70˚C for 5 min. After the mixture was allowed to cool on ice, 1 µl each of the pJET1.2 Cloning Vector (50 ng/µl) and T4 DNA Ligase were added on ice. The ligation mixture was then incubated at 22˚C for 30 min. The ligation mixtures were then transformed into Top Ten *E. coli* cells. Transformed cells were plated on Luria broth (LB) agar plates containing ampicillin (50 mg/ml) and incubated overnight at 37˚C.

Resultant clones were screened for the presence of desired inserts and sent off for commercial sequencing (MCLAB) using the pJET1.2 Forward (5'-CGA CTC ACT ATA GGG AGA GCG GC-3') and pJET1.2 Reverse (5'-AAG AAC ATC GAT TTT CCA TGG CAG-3') primers. Partial 16S rRNA gene sequences were manually trimmed of primer sequences using Se-Al version 2.0a11 Carbon (Rambaut, 1996). BLAST searches (http://blast.ncbi.nlm.nih.gov/) were used to determine close relatives of each operational taxonomic unit (OTU). Sequences

were aligned with the ClustalW aligner of the MEGA 5.0 program (Tamura, 2011). Maximum Likelihood trees were constructed and edited using the MEGA 5.0 program with the neighbour-joining method, the Juke-Cantor model option and a bootstrap value of 1000.

Pyrosequencing

Purified DNAs were diluted to a concentration of 20 ng/µl, of which a 20 µl aliquot from each sample was shipped to Molecular Research LP (Shallowater, Texas) for 16S rRNA Tag-Encoded FLX Amplicon Pyrosequencing (bTEFAP). A 25 µl PCR reaction using 16S universal Eubacterial primers 27F (5'-AGA GTT TGA TCM TGG CTC AG- 3') and 530R (5'-CCG CNG CNG CTG GCA CS- 3') was performed with a 5 min initial denaturing step at 95°C followed by 30 cycles of; 94°C for 30 s, 52°C for 40 s, 70°C for 40 s and a final extension step of 70°C for 5 min. Resultant amplicons were then mixed and purified using Agencourt Ampure beads (Agencourt Bioscience Corporation) and amplified by emulsion PCR. After recovery and enrichment, the bead attached DNAs were denatured with NaOH solution and sequencing primers were annealed. The 454 Titanium sequencing run was then performed on a 70x75 GS PicoTiter Plate using the Genome Sequencer FLX System (Roche). Raw data from the sequencing reactions were then returned digitally as Q25 .fasta and .qual files for further analysis.

Analysis Pipeline

The Q25 sequence data derived from the sequencing reactions was processed using a proprietary analysis pipeline (www.mrdnalab.com). Sequences were depleted of barcodes and primers then short sequences of less than 200 bp were removed. Sequences with ambiguous base

calls or homopolymer runs exceeding 6 bp were removed. These barcode and primer trimmed files were then further analyzed using the Quantitative Insights into Microbial Ecology (QIIME) open source software package on an Amazon EC2 Instance using Elastic Block Store (Caporoso, 2010). Sequences were analyzed based on the workflow shown in **Figure 3**. August 2012 samples resulted in a total of 231,898 sequences from the 454 pyrosequencing run. After quality filtering, 193,536 sequences were retained for further analysis. These sequences were between 250 and 550 bp with an average sequence length of approximately 400 bp. The number of sequences assigned to each sample ranged from 7,626 and 20,724. May 2013 samples resulted in a total of 228,444 sequences from the 454 pyrosequencing run. After quality filtering, 211,513 sequences were retained for further analysis. These sequences were between 250 and 673 bp with an average sequence length of approximately 458 bp. The number of sequences assigned to each sample ranged from 2,311 and 23,153.

Statistical analyses of variation between each sample were performed to validate the difference in community. The sample effect of depth versus carbon source composition was performed using the adonis and ANOSIM statistical programs. Each program employs a multivariate two-way comparison based on the selected treatment group. The R statistic and *p* value significances correlate to the amount of variation attributed to each treatment effect. ANOVA was used to determine the statistical difference between each sample at the class level.

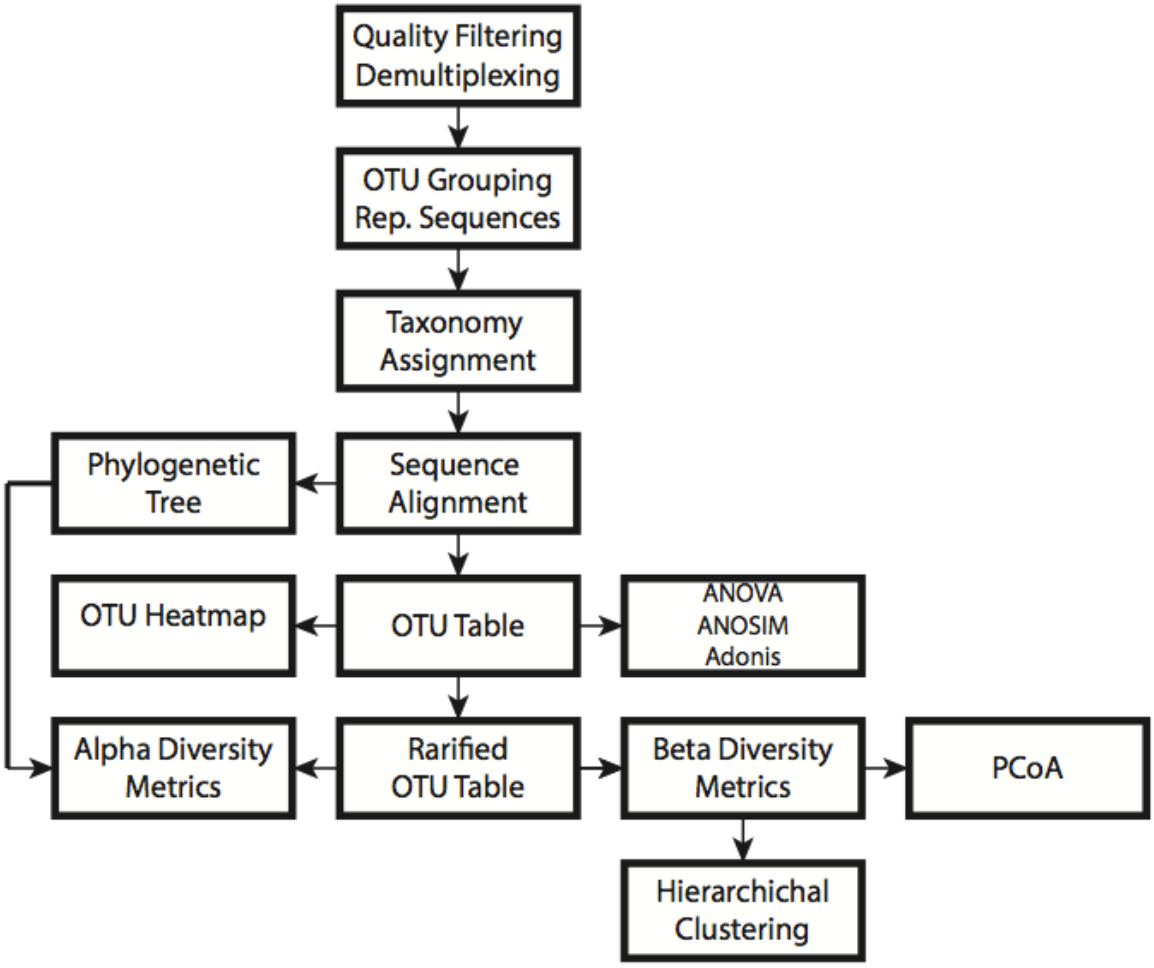

Figure 3 Workflow for QIIME 16S Pyrosequencing Analysis. Only sequences with a minimum quality score of 25, length between 200 and 1000 bps, no ambiguous bases and no mismatches in the primer sequence were used. Unifrac distance matrices were used for beta diversity analysis.

Quantitative Polymerase Chain Reaction

DNA extracted from each reactor port was used as template for quantification of 16S rRNA and *dsrB* gene copy number using quantitative PCR (qPCR). Primers Bac341F (5'-CCTACGGGAGGCAGCA-3') and Bac518R (5'-ATTACCGCGGCTGCTGG-3') were used for *Bacterial* 16S rRNA quantification (Li, 2012). The *dsrB* gene copy number was determined

using the primers DSR1F (5'-ACS CAC TGG AAG CAC G-3') and DSR4R (5'-GTG TAG CAG TTA CCG CA-3') (Foti, 2007). DNA was standardized to 15 ng/µl and 30 ng/µl for 16S and *dsrB* quantification after optimal dilutions were tested. Reactions consisted of 10 µl of SYBR® Green SuperMix (Quanta Biosciences), 1 µl of template DNA, 0.1 µM of each primer for the target gene, and nuclease free H_2O to a final volume of 20 µl. Reactions were loaded in triplicate along with a triplicate no template control on one half of a Low 96-well Clear Multiplate® PCR Plate™ (Bio Rad) and placed in an MJ MiniOpticon™ Thermocycler (Bio Rad). Baseline and threshold value calculations were performed using CFX™ Manager Software (Bio Rad). Cycling parameters for *Bacterial* 16S rRNA gene analysis were as follows: 95˚C for 3 min, followed by 40 cycles of 95˚C for 15 s and 55˚C for 30 s with a measurement taken after each cycle, followed by a melting curve period of 50˚C to 95˚C with a heating increment rate of 0.5˚C per 5 s (Li, 2012). Cycling parameters for *dsrB* gene analysis were as follows: 95˚C for 3 min, followed by 35 cycles of 95˚C for 40 s and 55˚C for 40 s with a measurement taken after each cycle, followed by a melting curve period like the 16S rRNA gene protocol (Foti, 2007). Standard curves for each gene study were generated using serial dilutions (10^8 to 10^2 copies) from a known quantity of purified *Desulfovibrio vulgaris* Hildenborough genomic DNA on the basis of each genome copy harboring five 16S rRNA gene copies and one copy of the *dsrB* gene.

CHAPTER 3

RESULTS

Geochemical Analyses

Temperature, pH, oxidation-reduction potential (ORP), and sulfate concentration were monitored bi-monthly using both field and laboratory techniques. As seen in **Figure 4**, temperatures of the Reactor Outflow ports were similar to the daily average ambient temperature throughout the course of the study. Initial temperature readings were between 25˚C and 22˚C throughout the first several months of the experiment. Temperatures of the effluent declined during the winter months (November-February) and steadily rose until the final May measurements as local temperatures began to rise with the change of season.

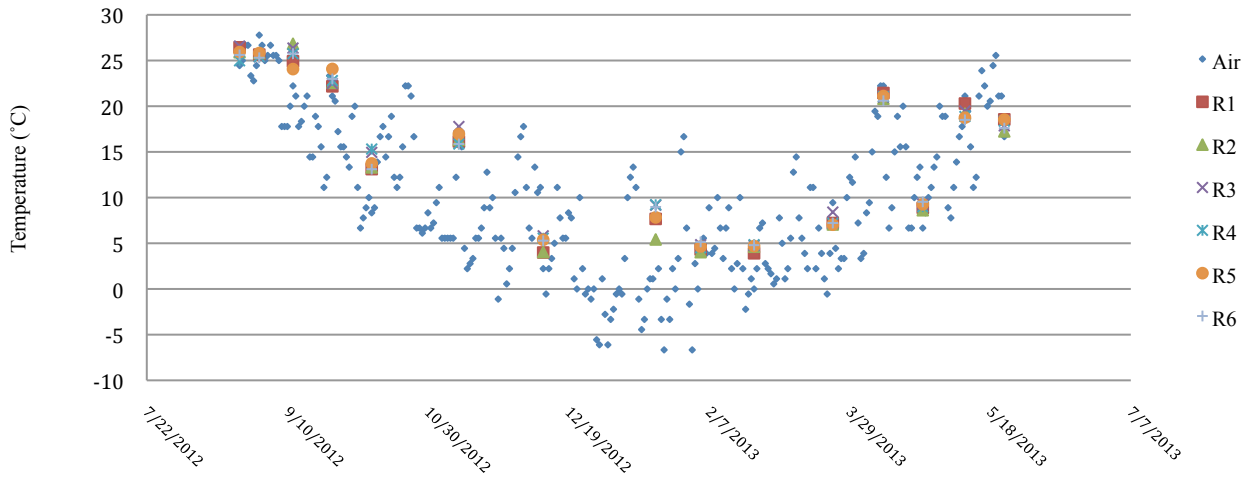

Figure 4 Bioreactor Outflow and Regional Temperature Temperatures from field measurements taken from the outflow ports of each reactor plotted alongside Southern Illinois daily average temperatures.

The pH of both the influent and effluent waters from each Bioreactor was tested on site throughout the length of the study and shown in **Figure 5** and **Figure 6**. The effluent pH initially ranged from 4-5, including the control reactor. However, in all substrate containing Bioreactors pH levels soon increased, while the pH in the control reactor declined to a value close to the

incoming AMD itself. **Figure 6** shows that initially the AMD pools above each Bioreactor were higher in pH than the incoming AMD from the stream as well as the AMD pool inside the control reactor (Bioreactor 1). Fluctuations occurred over the course of the experiment before the influent pool pH levels regressed to that of the AMD stream and Bioreactor 1. Despite this decrease in influent pH, the measured Outflow Ports containing substrate mixtures remained higher than the AMD influent. Bioreactors 3, 4 and 5 Outflow pH began to decrease in March 2013, continuing to decline until the final sample point in May. Bioreactor 2 and 6 Outflow pH values initially declined as well, but began to steadily increase in April, a trend which continued throughout the end of the study.

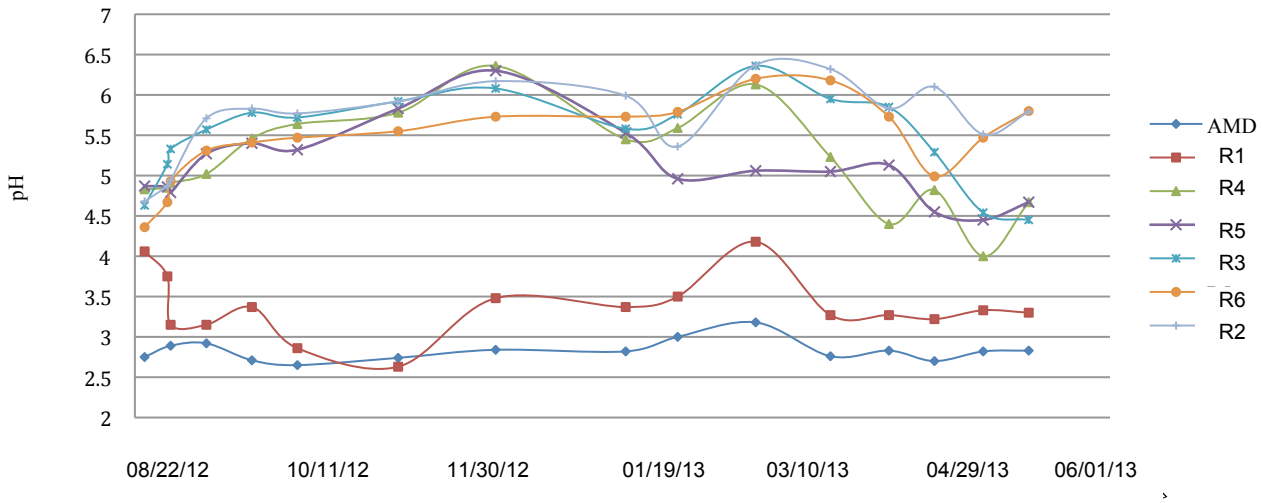

Figure 5 Bioreactor Effluent pH Values Field pH measurements of the effluent from the outflow port of each bioreactor. AMD influent pH values are shown as a reference.

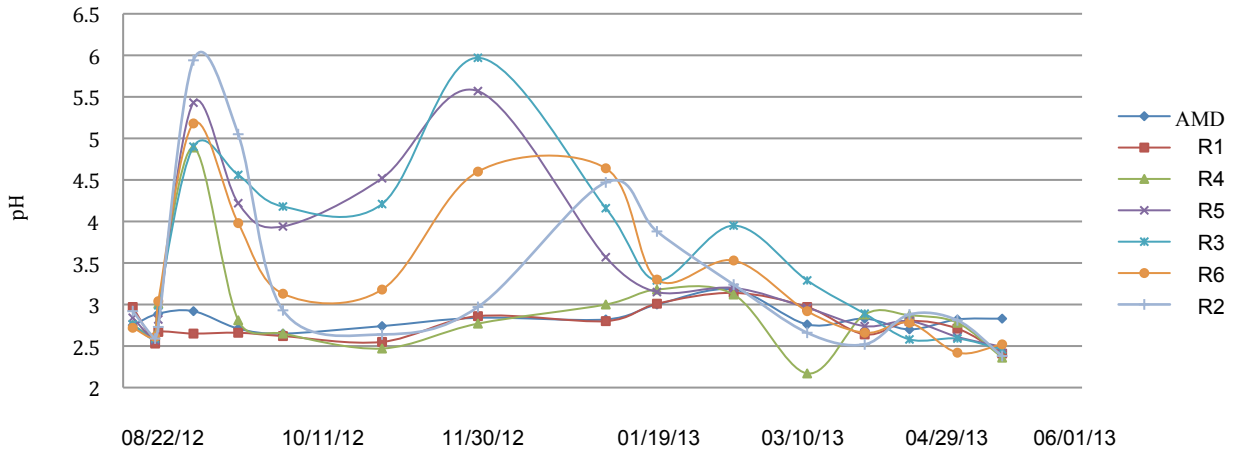

Figure 6 Bioreactor Influent pH Values Field pH measurements of AMD influent measurements for influent pH were taken from the collected AMD pools above the substrate layers.

ORP of the AMD influent as well as the effluent from the Outflow ports of each bioreactor was also monitored on-site throughout the course of the study. **Figure 7** shows the OPR data collected from August 2012 to May 2013. AMD influent and Bioreactor 1 effluent ORP values from August 2012 to February 2012 averaged 98 and 69 mV, respectively. ORP measurements began to climb in February and continued to increase until the study concluded, averaging 354 mV in AMD influent and 330 mV in the Bioreactor 1 Outflow during that time. Experimental Bioreactors (2-6) ORP values were negative within one week post-exposure to AMD and remained between -100 and -200 mV until December. After a steady increase in each Bioreactor Outflow from December through early March, ORP values began to decline to values below -100 mV, similar to the final measurements in early May.

Figure 8 shows the percent of sulfate removed by each bioreactor throughout the course of the experiment. Data shown was calculated using the amount of sulfate present in the outflows of each bioreactor subtracted from the sulfate concentration present in the acid pool above the substrate layer of each bioreactor. The bioreactors were effective at removing sulfate

for the first 5 months of the experiment. Up to 78% sulfate removal was detected in Bioreactor 2 effluent with the other experimental reactors in the range of 38-66% removal. As the temperature decreased however, sulfate removal decreased in all the bioreactors, with data suggesting a net increase in sulfate concentration after AMD exited Bioreactors 1 and 3. As temperatures rose and fell in early spring the same pattern was seen in the percent of sulfate removed by the bioreactors. As of May 2013, sulfate removal percentage of all the reactors, including the substrate lacking Bioreactor 1 looked to be increasing.

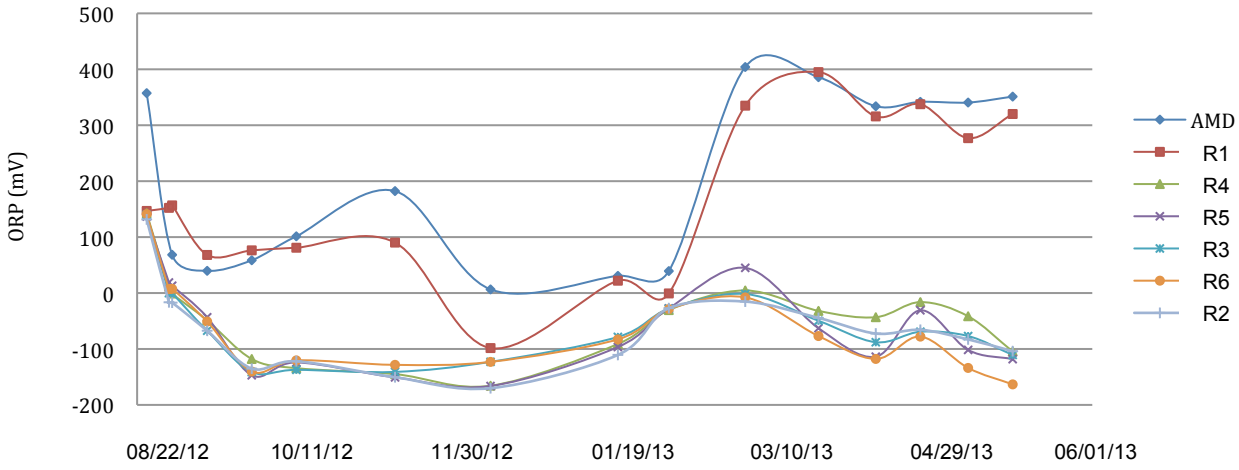

Figure 7 Bioreactor ORP Values Field measurements of bioreactor effluent and AMD influent ORP during the course of the study. ORP is shown in millivolts.

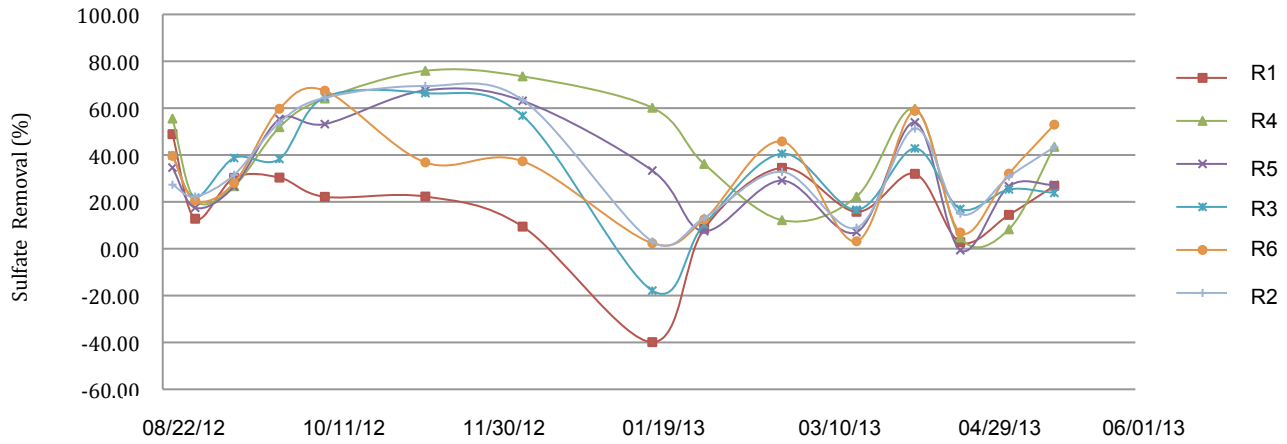

Figure 8 Bioreactor Percentage of Sulfate Removed Percent of sulfate removed from influent AMD to outflow effluents in each bioreactor.

Sulfate-Reducing Enrichments

In addition to molecular techniques used to characterize the bacterial community present in each bioreactor, traditional enrichment and isolation techniques were used to isolate sulfate-reducing bacteria (SRB). Enrichments from Port 3 of each substrate-containing bioreactor showed signs of sulfate reduction approximately ten days after inoculation. After several rounds of dilutions and plating, enrichments from Reactor 3 (70:30 complex:simple substrate ratio), showed distinct colony formation which were either cream or black in color on medium containing 40 mM pyruvate (pH 5.5). These colonies also had a distinct hydrogen sulfide odor upon removal of liquid media from the anaerobic chamber. Five colonies were chosen for sequence analysis prior to being cryo-cultured. Isolates B3-21 and B3-32 were most closely related to members of the genus *Desulfovibrio* based on partial 16S rRNA gene sequence as shown in **Figure 9**. The tree shown has the highest log likelihood (-1265.5360) of the 1000 trees analyzed in tree space. Isolate B3-21 appeared most closely related to *D. desulfuricans* with 98%

sequence identity within the 16S region analyzed. *D. multispirans* appeared to be the most closely related cultured organism to isolate B3-32, with 99% sequence identity within the analyzed region. The physiology, particularly substrate utilization capability and growth rate of these strains are currently being investigated.

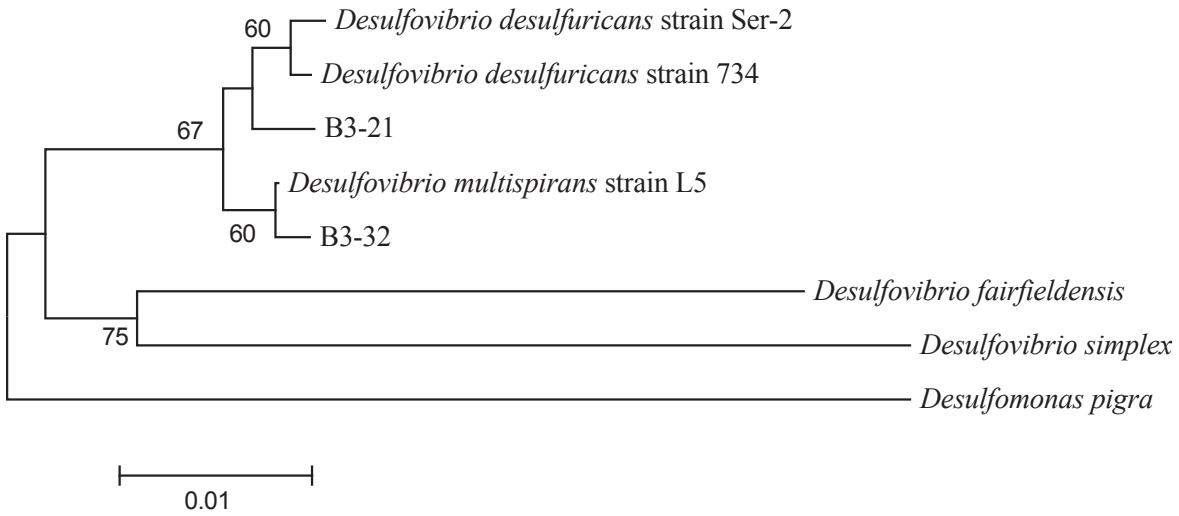

Figure 9 Phylogenetic Tree of *Desulfovibrio* Related Isolates Maximum Likelihood tree of partial 16S rRNA gene sequences related to *Desulfovibrio* species aligned with ClustalX© and constructed using MEGA 5.0© software using the Jukes-Cantor model (Tamura, 2011). The percentage of trees in which the associated taxa clustered together is shown next to the branches. Scale bar represents base changes per site.

Besides *Desulfovibrio* species, organisms affiliated with complex substrate utilization were also isolated. **Figure 10** shows the most likely tree representing the phylogenetic relationships of the *Clostridium* like isolates with their closest cultured relatives. The log likelihood of this tree, -2328.3638, is the result of the much larger differences of the sequences represented within. Isolate B3-24 showed 90% sequence identity to *Sporanaerobacter acetigenes*, the most closely related species based on the tree phylogeny. The phylogenetic relationship of isolate B3-35 was not fully resolved based on the length of sequence analyzed. However, it did group confidently with *C. thiosulfatireducens* and *C. sulfidigenes,* two very

closely related members of the *Clostridium* genus. *C. sulfidigenes* was the closest relative of B3-35 based solely on sequence similarity, sharing 99% 16S sequence identity within the analyzed region. The same can be said of isolate B3-30, which was most closely related to either *Anaerovorax odorimutans* or *C. aminobutyricum* based on phylogeny of the analyzed region. Based on strict sequence similarity however, B3-30 was more closely related to *C. aminobutyricum* (96%) than *A. odorimutans* (93%).

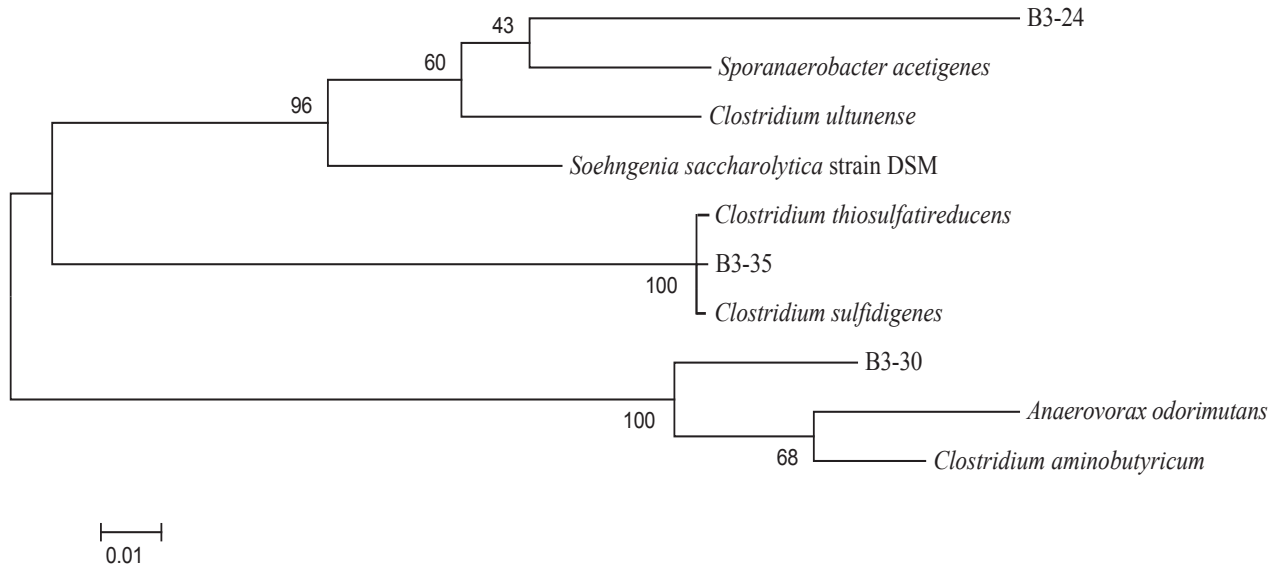

Figure 10 Phylogenetic Tree of *Clostridium* Related Isolates Maximum Likelihood tree of partial 16S sequences related to *Clostridium* species aligned with ClustalX and constructed using MEGA 5.0 software using the Jukes-Cantor model (Tamura, 2011). The percentage of trees in which the associated taxa clustered together is shown next to the branches. Scale bar represents base changes per site.

Fluorescent *in situ* Hybridization (FISH)

To determine the relative abundances of *Betaproteobacteria*, *Deltaproteobacteria*, *Alphaproteobacteria*, and *Acidobacteria* present in each bioreactor at the beginning of the field experiment, samples were collected in August of 2012 and analyzed using FISH. Samples from Ports 1 and 2 as well as Port 3 and the Outflow of each reactor were combined and tested with

each probe in order to determine the differences in microbial community based on both sample depth and substrate composition. The total abundance of bacterial cells when compared to all DAPI stained cells ranged from 86%-92%. Relative abundances for more specific probes are seen in **Figure 11**.

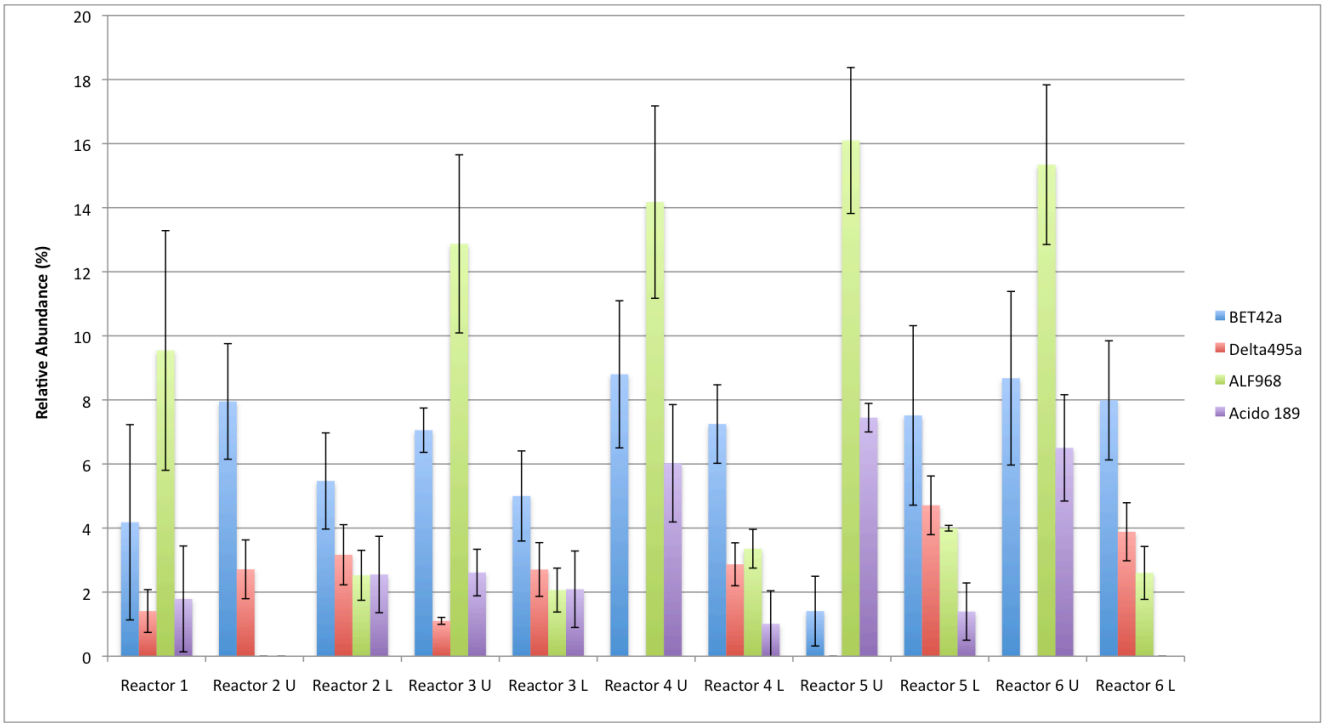

Figure 11 Relative Abundances Determined by FISH Percentage of cells detected by each probe relative to the total bacterial cell count. Cell counts for the two upper ports (1 and 2) and two lower ports (3 and Outflow) are denoted by U and L, respectively. No data were attained for ALF968 and Acido 189 probes for samples from the upper ports of Reactor 2. Error bars represent 1 standard deviation.

Relative abundances for *Betaproteobacteria*, as determined by probe BET42a ranged from 1.4% (Reactor 5 U) to 8.8% (Reactor 4 U). A range of 0% (Reactor 5/6 U) to 4.7% (Reactor 5 L) was seen for *Deltaproteobacteria* as determined by probe Delta495a. Probe ALF968 targeting *Alphaproteobacteria*, showed the largest abundance range, from 2.1% (Reactor 3 L) to 16.1% (Reactor 5 U). Relative abundances for *Acidobacteria* ranged from 1.0% (Reactor 4 L) to 6.5% (Reactor 6 U) as determined by probe Acido 189. Any relative abundance

with a value of zero was not higher than the percent of cells hybridized by probe NON 338. Due to the time constraints of this project, FISH was not performed on samples from May 2013.

Pyrosequencing Analysis

August 2012 Samples

To obtain a snapshot of the bacterial community present in the bioreactors, DNA samples from each time point sampled were analyzed using for 454 pyrosequencing (Molecular Research LP). **Figure 12** shows the relative abundance at the class level for the operational taxonomic units (OTUs) represented in the sequencing data set. The three ports sampled from Bioreactor 1 had very similar community profiles, with members of the *Acidobacteria* representing between 39-49% of the sequences from each port. *Betaproteobacteria* were also prevalent, representing 24-31% of the sequences from the control Bioreactor. Bioreactor 2 Port 2 sequences were comprised mostly of *Alphaproteobacteria* and *Bacilli*, representing 37.1% and 46.4% of sequences, respectively. *Clostridia* and *Bacilli* dominated the lower ports, Port 3 and the Outflow port, with the two classes accounting for virtually all of the sequence distribution therein. Bioreactor 3 showed a similar sequence distribution, however Port 2 samples contained a higher number of sequences similar to *Bacilli* (73.8%) and a smaller proportion of members of the *Alphaproteobacteria* (9.5%). Bioreactor 3 Port 3 sequences were distributed between 3 classes: *Bacteroidia* (36.2%), *Clostridia* (32.0%), and *Bacilli* (30.1%). The Outflow of Bioreactor 3 was similar to that of Bioreactor 2, consisting almost entirely of members of *Bacilli* (76.3%) and *Clostridia* (23.1%). The sequence distribution of Port 2 samples from Bioreactors 4, 5, and 6 were all relatively similar. In each case, sequences similar to *Alphaproteobacteria* (46-60%)

were the most abundant, while *Bacilli* (23-30%) were also well represented. Samples from Port 3 for Bioreactors 4 and 5 were also similar, with *Bacilli*-like sequences the most abundant (71.5% and 74.3%). Bioreactor 6 Port 3 sequences were predominantly from the class *Clostridia* (64.3%). *Clostridia* and *Bacilli* sequences were most prevalent in the Bioreactor 4 Outflow, constituting 77.5% and 18.6% of the sequenced community, respectively. *Bacteroidia* and *Clostridia* sequences were prevalent in the lower ports of Bioreactor 5 and 6. *Bacteroidia* sequences accounted for 55.4% of the sequences in Bioreactor 5 Outflow and 21.6% in Bioreactor 6 Port 3. Bioreactor 5 and 6 Outflow communities were comprised of 39.9% and 64.3% *Clostridia* sequences, respectively.

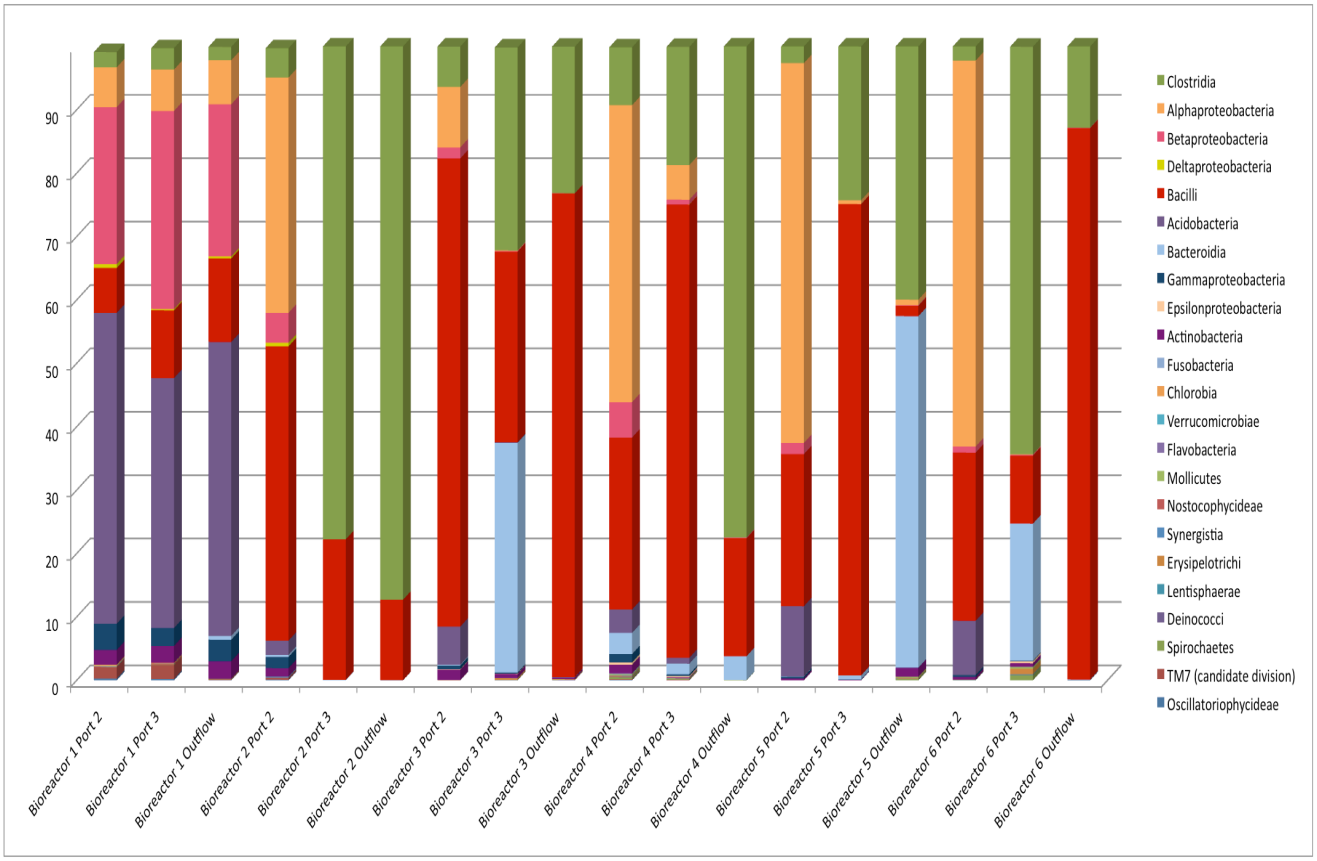

Figure 12 Relative Bacterial Class Abundance from August 2012 Relative class abundance from each sample reactor port based on OTUs chosen at a 97% sequence similarity cutoff.

Sampling depth and within sample diversity (alpha-diversity) measures were carried out to determine the diversity of the microbial community within each bioreactor. Rarefaction curves for observed OTUs and Faith's Phylogenetic Diversity (PD) are shown in **Figure 13** (A and B). The observed OTU curve can be used to estimate if the sequencing effort was sufficient to capture the majority of OTUs present from the sampled environment. The Faith's PD curves can be used as an estimate of phylogenetic diversity based on the summation of the branch lengths from the phylogenetic trees that were constructed based on sequences found in each sample (Faith, 1992). Bioreactor 4 Port 2 had the highest PD value (113.1) at the highest tested sequencing depth (10,750 sequences), however it also had the highest slope (0.14) on the observed OTU curve, indicating that the diversity of species may still be underrepresented. Not surprisingly, Bioreactor 4 Port 4 also has the highest Shannon diversity value and Chao1 estimated richness, 6.9 and 2448, respectively (**Figure 14 A** and **B**). In contrast, Bioreactor 2 Outflow showed the lowest slope in Figure 10A (0.035), indicating the best sequencing depth of all samples while also having the lowest Faith's PD value of only 15.54. Bioreactor 2 Outflow also had a Shannon diversity score of 2.70 and a Chao1 estimate of only 481, the lowest of all samples in both cases. In most samples, higher values on the observed OTUs curve were indicative of a higher Faith's PD value, Shannon diversity score and higher Chao1 estimate being seen from the given sample. Samples from Bioreactor 1 as well as Bioreactor 3 and 6 Outflow were exceptions, with each Shannon diversity score relatively high despite a low Chao1 richness estimate.

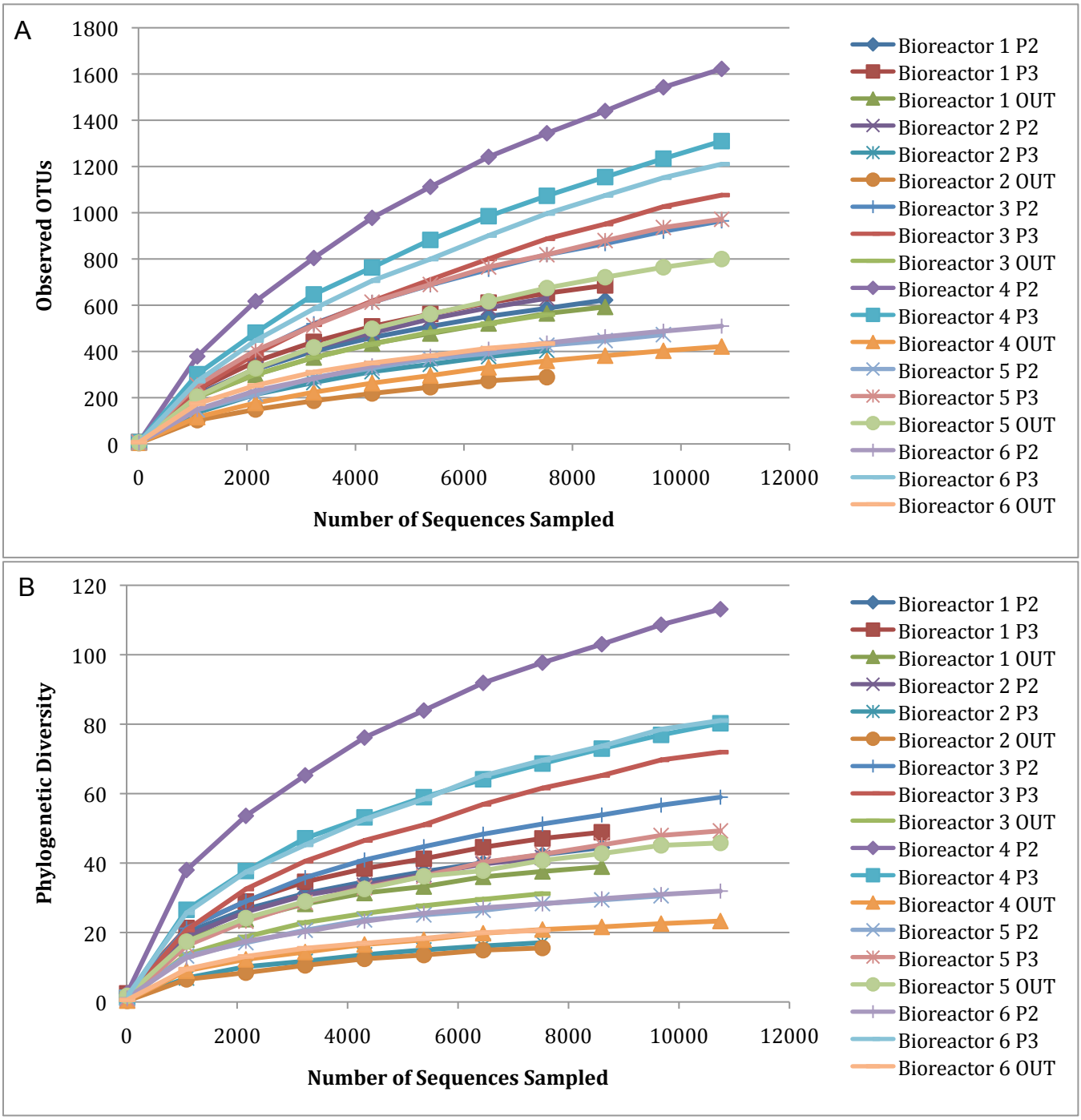

Figure 13 Rarefaction Analyses for August 2012 Sample Data Plots of (A) Observed OTUs and (B) Faith's PD metric values from rarified OTU tables. Port 2 (P2), Port 3 (P3), and Outflow (OUT) data are shown.

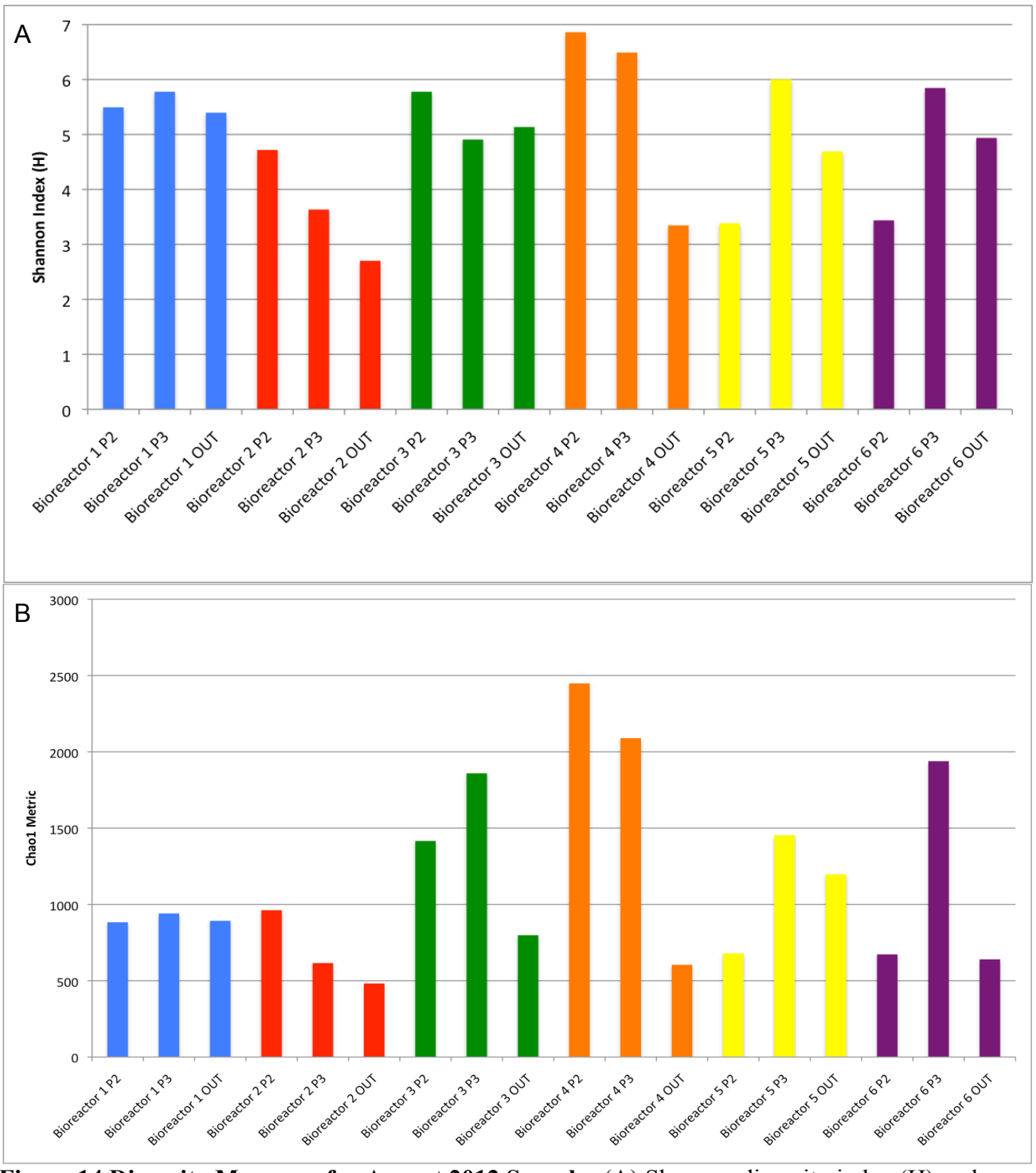

Figure 14 Diversity Measures for August 2012 Samples (A) Shannon diversity index (H) and (B) Bias-corrected Chao1 richness metric for all Bioreactor samples from August 2012 rarified to 7528 sequences. Shannon diversity reported as bits (log_2). Port 2 (P2), Port 3 (P3), and Outflow (OUT) data are shown.

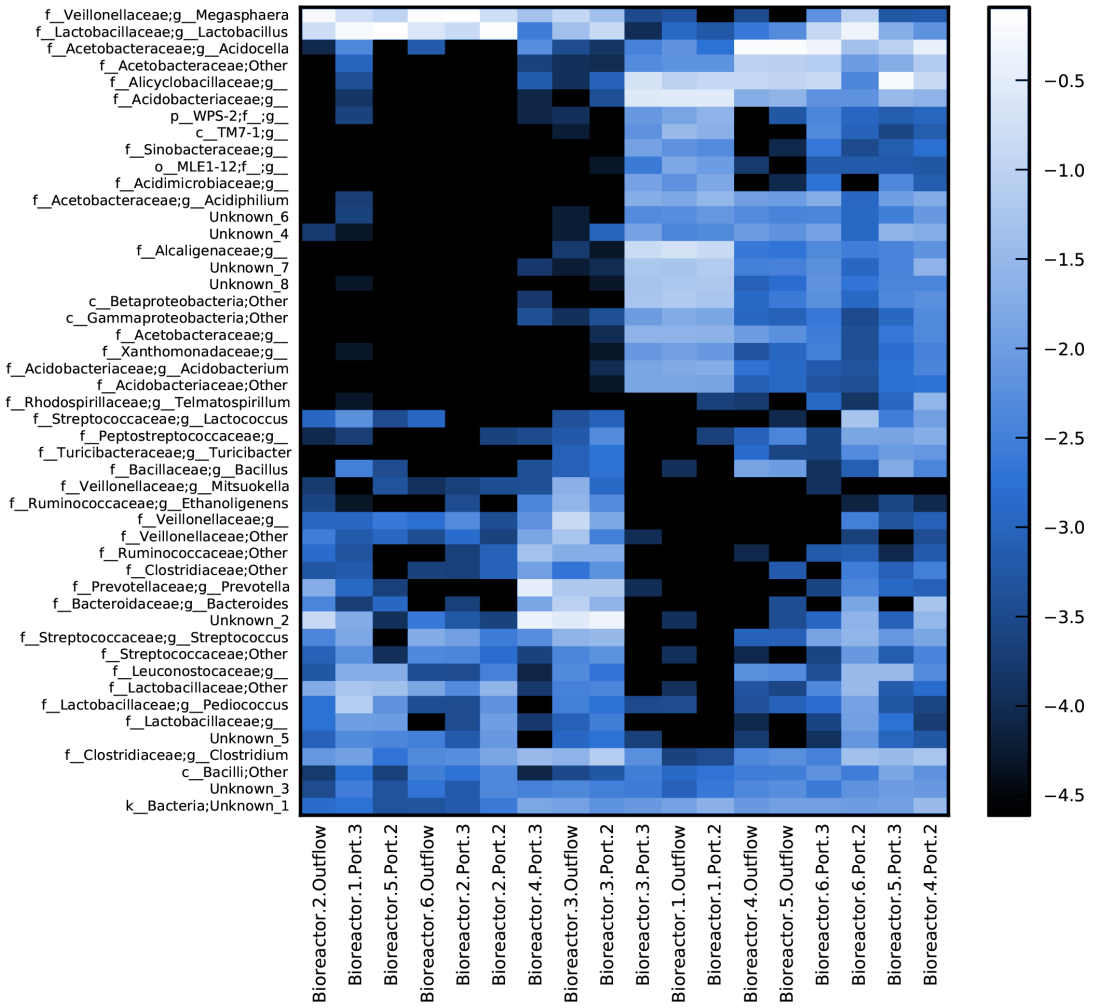

Figure 15 Genus Level Heatmap for August 2012 Samples Heatmap displaying OTUs at the genus level representing at least 0.125% of the total sequence abundance. OTUs are clustered by sequence similarity and colored based on an inverse log scale. OTUs without a genus could not be discerned to that phylogenetic level.

Figure 15 shows the relative sequence abundance at the genus level. The most abundant OTUs were similar to the genera *Megaspharea* and *Lactobacillus* belonging to the *Clostridium* and *Bacilli* classes, respectively. Each of these OTUs represented substantial portions of the total sequence pool in Bioreactor 2 as well as Bioreactor 1 and 5 Port 2 samples and the Outflow of Bioreactor 6. Sequences similar to *Acidocella* were prevalent in several Outflow samples. *Clostridium* and lactic acid bacteria sequences were present in high abundance within all

sampled ports. *Alicyclobacillaceae* and *Acidobacteriaceae* were essentially absent in most ports, but among the most abundant sequences in Bioreactor 3 Port 3 and Bioreactor 1 Port 2 and Outflow.

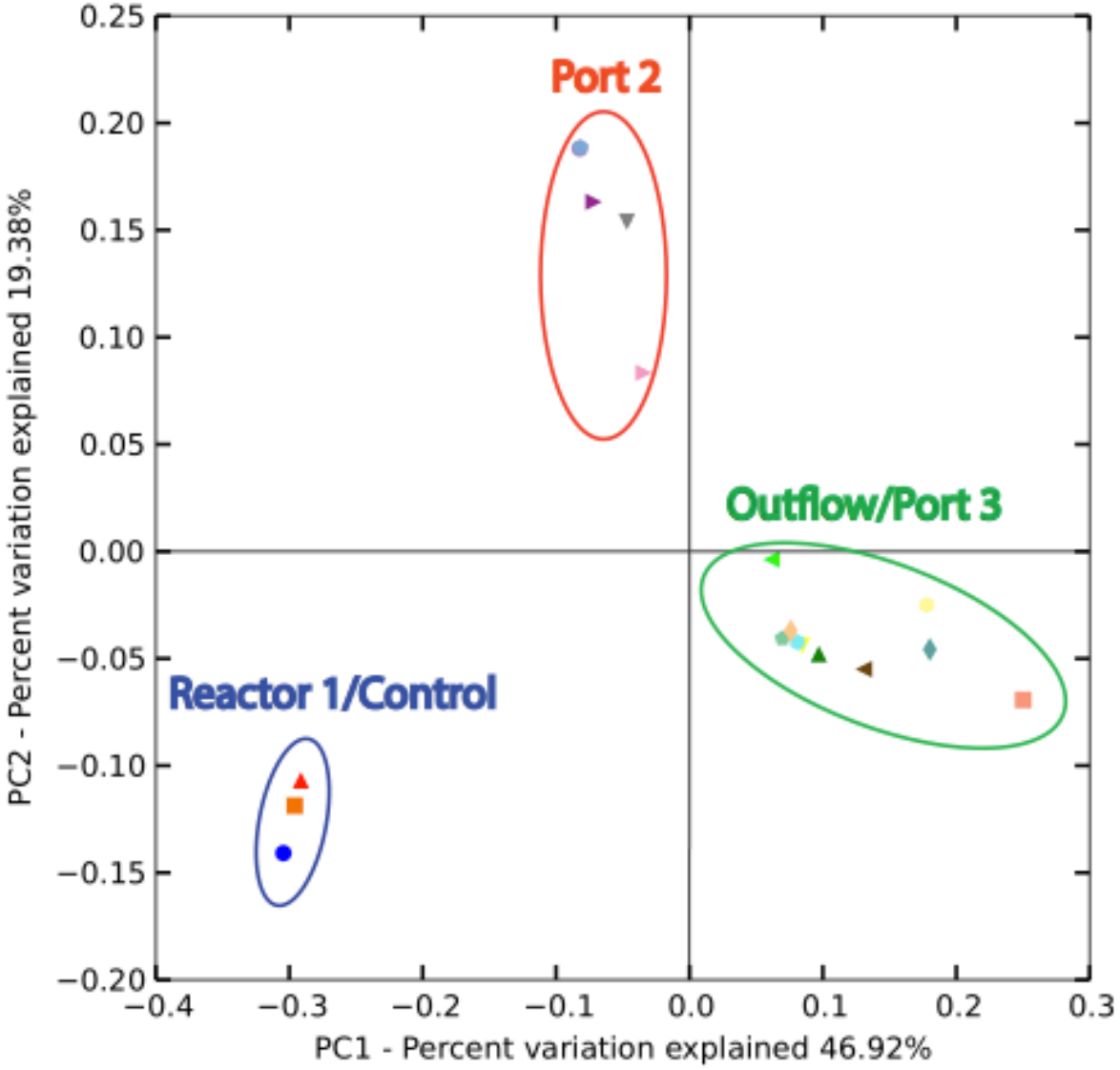

Figure 16 Principal Coordinate Analysis of August 2012 Samples PCoA scatter plot using the first and second eigenvalues as axes. Eigenvalues were calculated from weighted UniFrac distance matrices of each sample data set.

Several methods were used to examine the diversity between each barrel (beta-diversity) between each of the samples from August 2012. Principal Coordinate Analysis (PCoA) was

performed to determine the amount of the effect of the largest strings of data from weighted UniFrac distance matrices on each of the samples. **Figure 16** displays a 2-dimensional coordinate map of the first and second principal coordinates, PC1 and PC2, respectively. The PC1 axis represents 46.92% of the variation between samples, while PC2 accounts for 19.38%. Clear groupings were seen based on the depth of sample within substrate containing bioreactors. All of the control samples from Bioreactor 1 clustered together away from the experimental samples. The other samples clustered by depth, with the lower ports (Port 3 and Outflow) grouping together and the experimental Port 2 samples forming their own distinct cluster.

Figure 17 shows the same data as Figure 16 plotted in a 3-dimensional scatter plot. PC1 and PC2 from Figure 12 remained the same in addition to a third principal coordinate, PC3, which represents 17% of the sequence variation. The clustered groups remained the same, with Bioreactor 1 samples forming a distinct cluster while the experimental Port 2 samples clustered together away from the Port 3 and Outflow clusters. While Bioreactor 3 Port 2 clusters further from the other Port 2 samples, the 3-dimensional PCoA plot along with its placement on the PC1 axis indicate a definite clustering with other Port 2 samples.

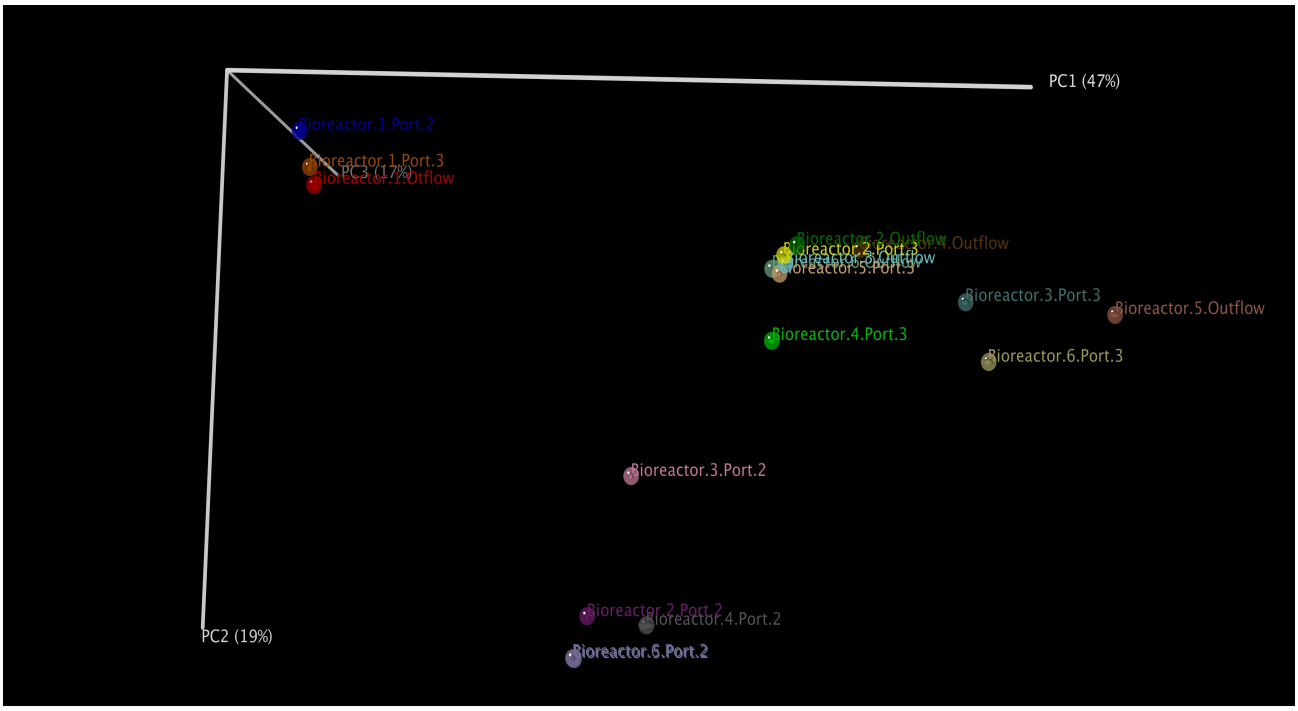

Figure 17 3D PCoA Scatter Plot of August 2012 Samples 3-dimensional scatter plot of PCoA plotted against the first, second, and third eigenvalues. Eigenvalues were calculated from weighted UniFrac distance matrices of each sample set.

A final beta-diversity test, a hierarchical clustering tree based on the Unweighted Pair Group Method with Arithmetic mean (UPGMA), was performed to show the clustering after jackknifed support (i.e., repeated resampling of the data from each sample). **Figure 18** shows the resultant jackknife supported UPGMA hierarchical clustering with support level coded by color. There is strong support clustering the Port 2 samples from the Port 3 and Outflow samples with the exception of Bioreactor 4 Port 3, which clustered with moderate support with Port 2 of Bioreactor 4. Bioreactor 1 samples were clustered together with high support while clustering more closely to the Port 2 samples than Port 3.

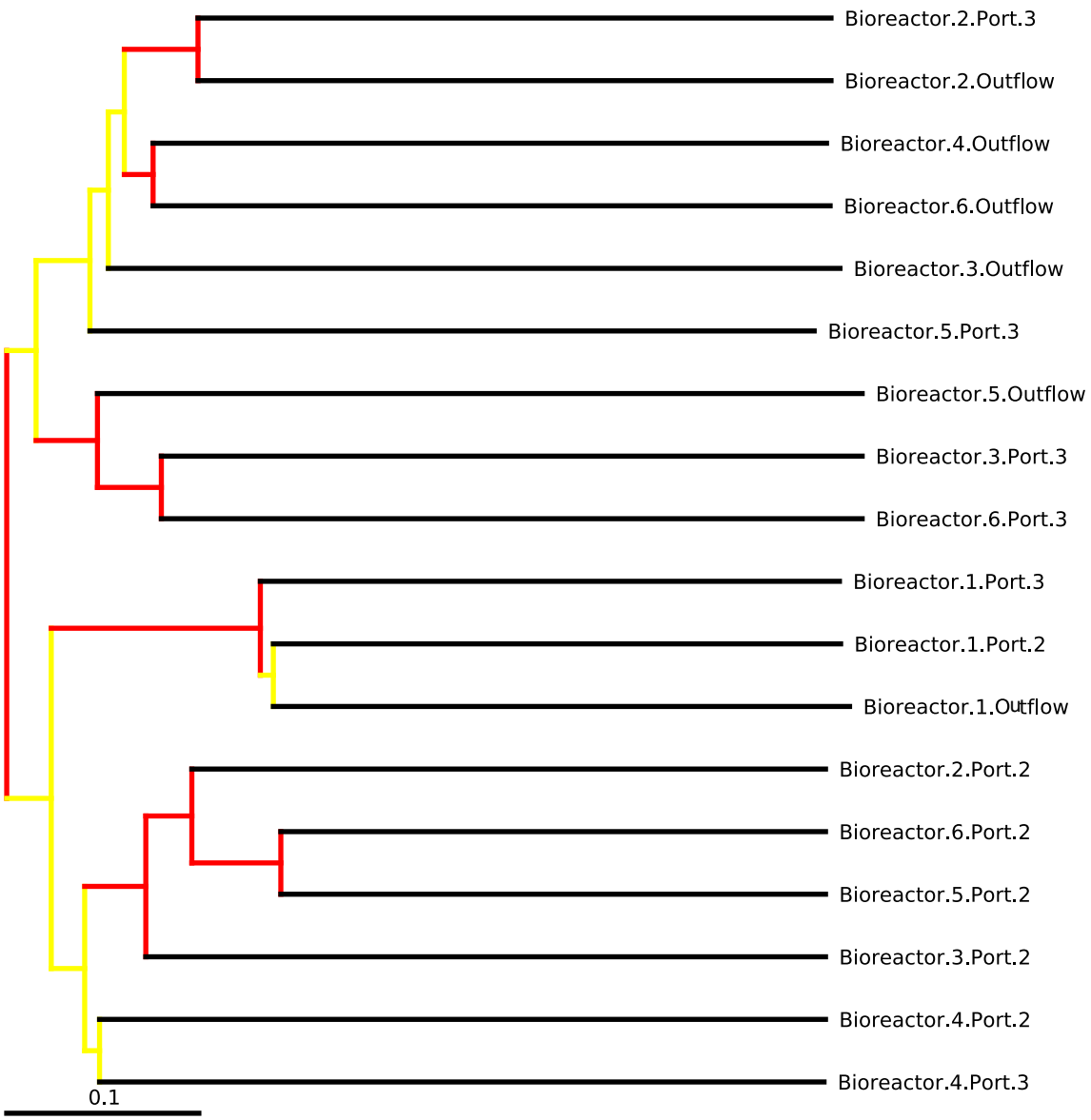

Figure 18 August 2012 UPGMA Hierarchical Cluster Tree Unweighted Pair Group Method with Arithmetic mean hierarchical clustering tree. Tree was constructed using UniFrac distance matrices. Tree node colors indicate jackknife support levels of 75-100% (Red) and 50-75% (Yellow). Scale bar represents branch length changes per distance matrix site.

May 2013 Samples

To determine how the initial bacterial community changed within each of the bioreactors over time, all analyses performed on the August samples were also performed on samples collected after 10 months of exposure to *in situ* AMD. Inhibition of the 454-sequencing run prevented a useable amount of data from being generated for Bioreactor 4 Outflow, thus that sample was excluded from all analyses. **Figure 19** shows the relative abundance at the class level of each sample from the second sampling effort. In the control reactor, Bioreactor 1, a large increase in the sequence representation of several classes was seen. Most notably, sequences similar to *Gammaproteobacteria* increased from between 2-4% in August 2012 to 39-46% in May 2013. *Acidobacteria* sequences decreased from 39-42% within Bioreactor 1 to 14-20% after ten months. *Alphaproteobacteria* sequences increased by approximately 6% in each of the ports, while *Betaproteobacteria* sequences decreased by 16-24% over the course of the study.

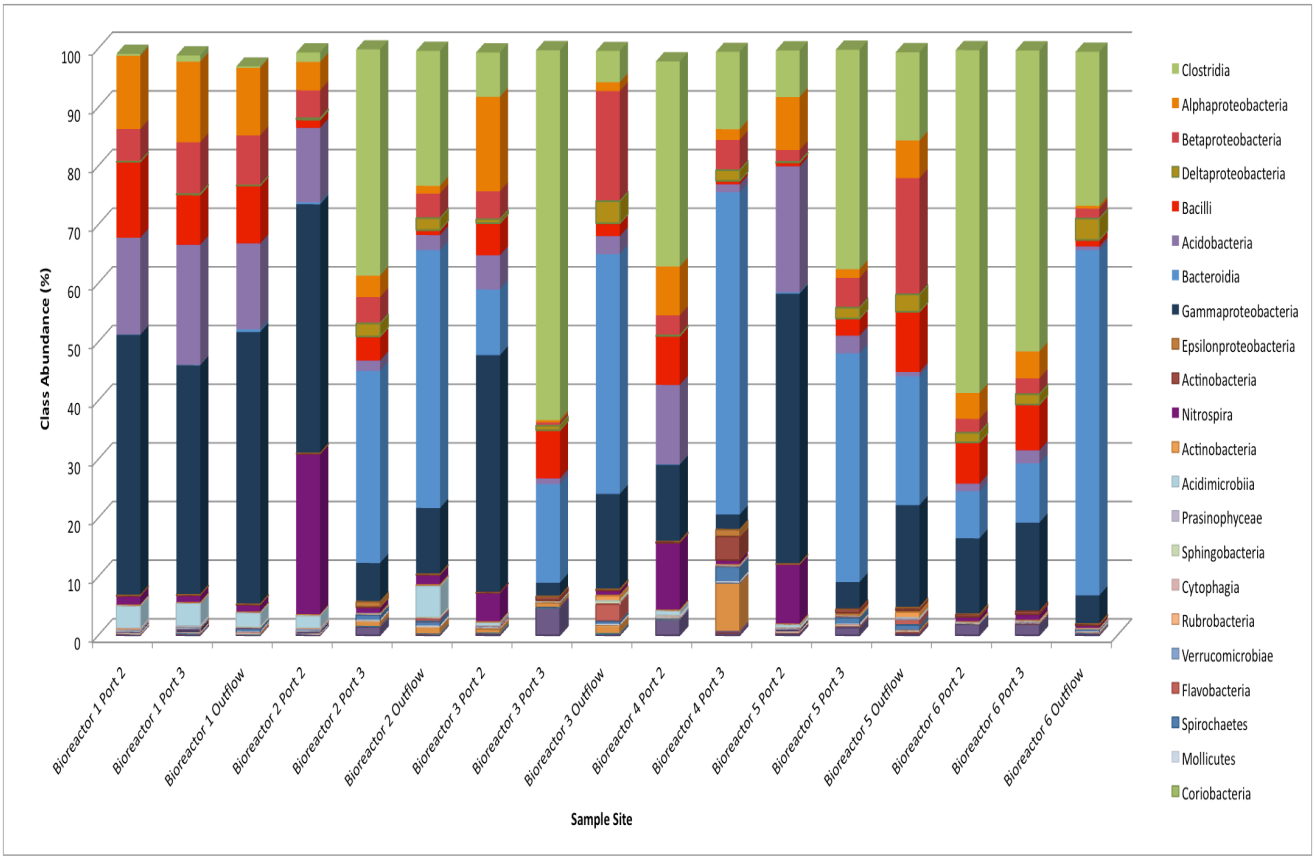

Figure 19 Relative Bacterial Class Abundance from May 2013 Relative class abundance from each sample reactor port based on OTUs chosen at a 97% sequence similarity cutoff. No data were attained from the Bioreactor 4 Outflow sample on the first 454-sequencing attempt.

In the experimental bioreactors, sequences from the *Gammaproteobacteria* class increased universally from August 2012 to May 2013. Port 2 samples from Bioreactors 2, 3, and 5 had the largest increases, with *Gammaproteobacteria* sequences representing 42.46%, 40.44%, and 46.1% of the sequence abundance, respectively. The relative abundance of *Bacteroidia* sequences also increased in the majority of the experimental samples. In particular, *Bacteroidia* sequences were the most prevalent class represented in the samples from the lower ports of Bioreactor 2, the Outflows of Bioreactor 3 and 6, as well as the Port 3 samples of Bioreactors 4 and 5. *Clostridia* sequences were still well represented, although not as prevalent as in most August 2012 samples. While the majority of samples showed a decrease in the relative

abundance of *Clostridia* sequences, Port 3 samples from Bioreactors 3 and 6 showed marked increases to 63.0% and 58.4% of their respective relative abundances compared to the August 2012 samples. *Bacilli* sequences also saw a near universal decrease during the course of the study. The relative abundance of *Bacilli* sequences decreased from 70-86% for several samples from August 2012, to a maximum of 10.3% in May 2013, with most samples containing only 5-8%.

Rarefaction curves for May 2013 samples are shown in **Figure 20 A**. Observed OTU curves were less level as they approached the right end of the curve for the second round of sequencing. The slopes of the curves ranged from 0.178-0.118, with Bioreactor 6 Port 2 and Bioreactor 2 Outflow having the greatest and least slopes, respectively. Not surprisingly, the Faith's PD values, as shown in **Figure 20 B**, were higher overall for samples from May 2013. Most notably, Ports 2 and 3 of Bioreactor 6 had PD values over 120, where only Bioreactor 4 Port 2 had a PD value over 100 in August 2012 samples. Also, Outflow ports from each Bioreactor had similar PD values and were grouped at the lower end of the PD value curves at 75.

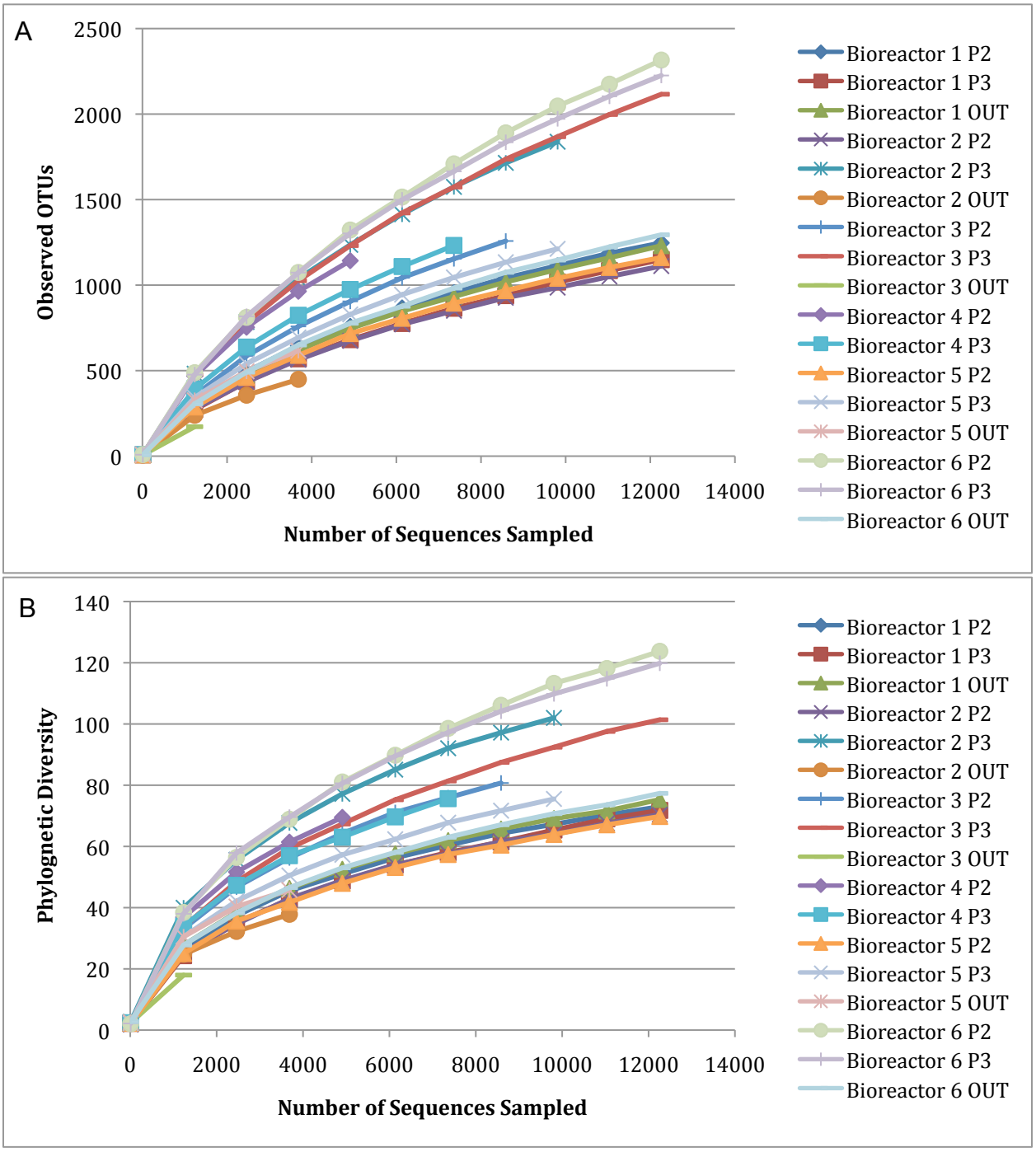

Figure 20 Rarefaction Analyses for May 2013 Sample Data Plots of (A) Observed OTUs and (B) Faith's PD metric values from rarified OTU tables. Port 2 (P2), Port 3 (P3), and Outflow (OUT) data are shown.

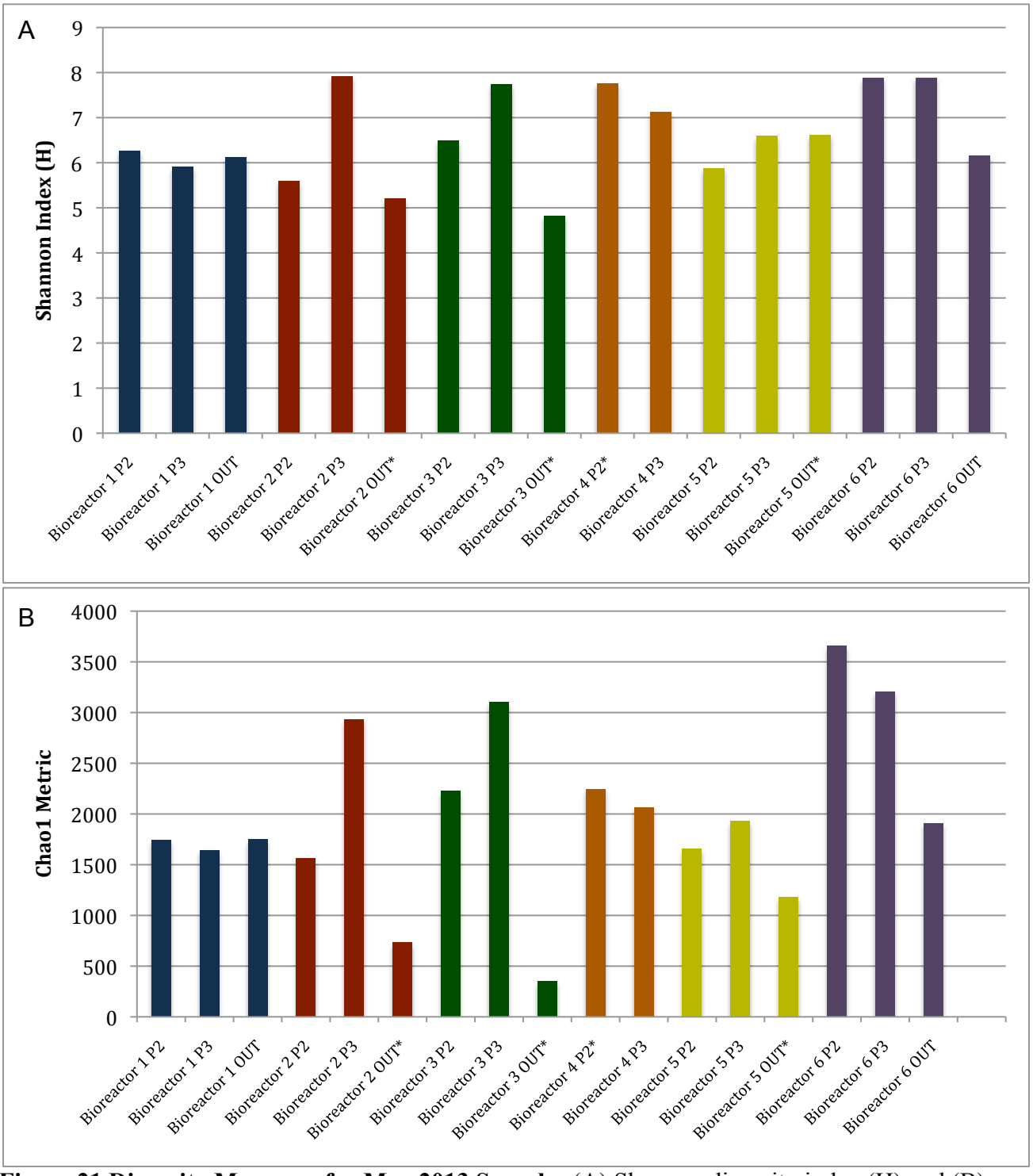

Figure 21 Diversity Measures for May 2013 Samples (A) Shannon diversity index (H) and (B) Bias-corrected Chao1 richness metric for all Bioreactor samples from May 2013 rarified to 7360 sequences. Shannon diversity reported as bits (log_2). Port 2 (P2), Port 3 (P3), and Outflow (OUT) data are shown. * Indicates samples with fewer than 7360 sequences.

Shannon diversity index calculations, shown in **Figure 21 A**, were also higher overall than those from the August 2012 samples (Fig. 11 A). Shannon diversity indicated that the Port 3 samples from Bioreactors 2, 3, and 6 along with Port 2 samples from Bioreactors 4 and 6 were the most diverse with H values very close to 7.9. Outflows from Bioreactors 2 and 3 had the lowest estimated diversity, with H values of 4.8 and 5.2, respectively: although it should be noted that these numbers represent calculations performed with fewer than the 7,360 sequences used for the other samples. Richness estimates by the Chao1 index are shown in **Figure 21 B**. Bioreactor 6 Ports 2 and 3 had the highest estimated richness. Followed by Bioreactor 3 Port 3. The lowest estimated richness values were seen in the Outflow samples from Bioreactors 2, 3 and 5, which were the samples with fewer sequences. Of the samples with the full compliment of sequences, Bioreactor 1 samples and the Port 2 samples of Bioreactor 2 and 5 were the lowest, ranging from 1,566-1,749 estimated species.

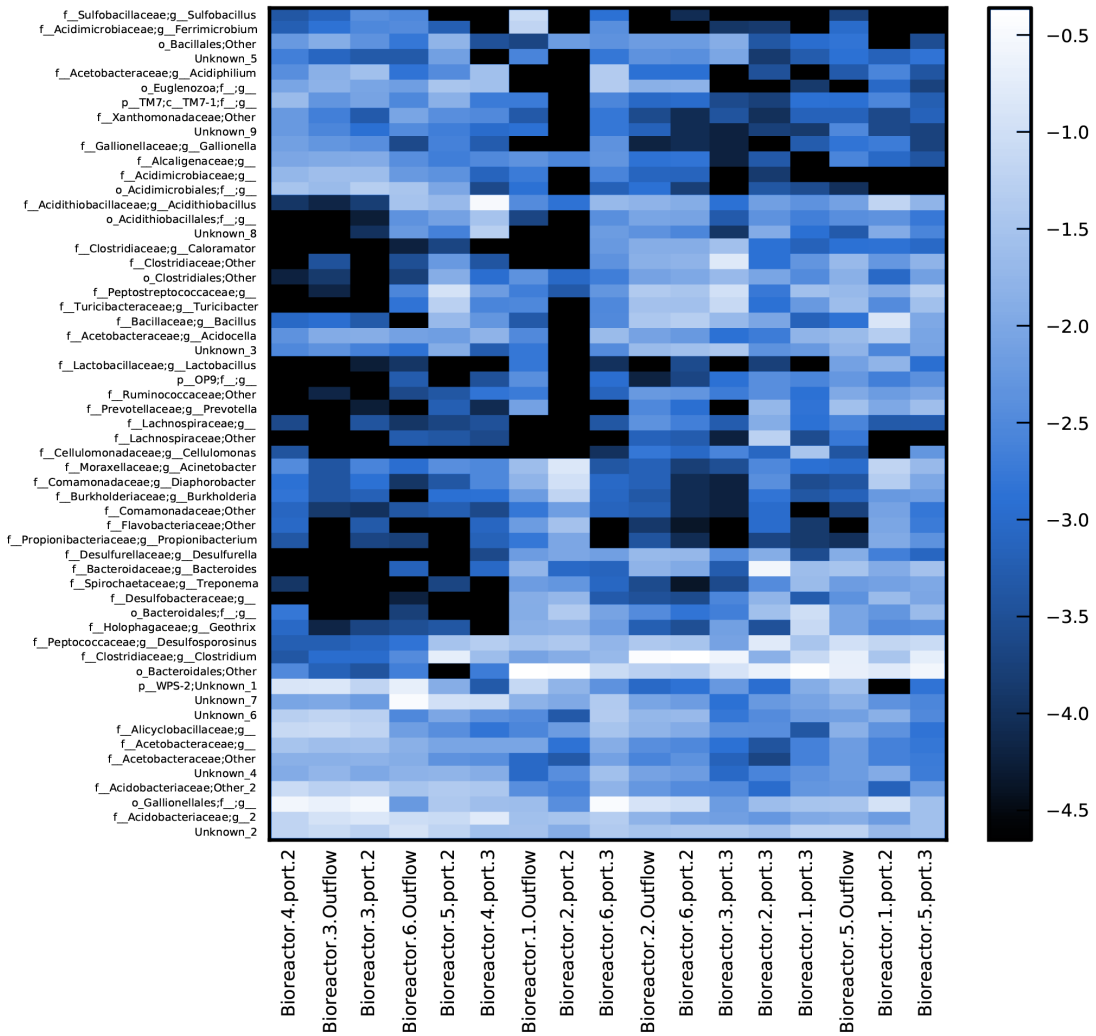

Figure 22 Genus Level Heatmap for May 2013 Samples Heatmap displaying OTUs at the genus level representing at least 0.125% of the total sequence abundance. OTUs are clustered by sequence similarity and colored based on an inverse log scale. OTUs without a genus could not be discerned to that phylogenetic level.

A hierarchical clustering Heatmap displaying data gathered from the May 2013 samples is shown in **Figure 22**. Most notably, members of the *Desulfurella* and *Desulforospinus* were found in many of the experimental Bioreactor samples. *Acidithiobacillus* species were present in significant quantities in each of the samples. Members of the *Clostridia* and *Bacillus* genera were still highly abundant throughout all of the samples, although not as dominant as in the

August 2012 samples (Fig. 12). Overall, the samples were more diverse at both the class and OTU level in the May 2013 samples than the August 2012 samples (Figs. 9, 12, 16, 20).

Principal coordinate analysis results are shown in **Figures 23** and **24**. In this analysis PC1 represented 44.2% of the variation, PC2 represented 20.4% of the variation, and PC3 represented 8.3%. Clear clusters were not as obvious in the May 2013 samples as they were in the August 2012 samples. Samples from Bioreactor 1 clustered closely together, although several Port 2 samples also clustered closely. The 3D PCoA plot shows a distance between the Bioreactor 1 samples and the Port 2 samples based on the PC3 axis. While no distinct clusters formed, experimental Outflow samples were clustered more closely together with each other and with the majority of Port 3 samples. However, the Port 3 samples from Bioreactor 3 and 6 were distant from the rest of the Outflow and Port 3 samples. Interestingly, Bioreactor 6 Ports 2 and 3 appear to form a cluster of their own, made more apparent in the 3-dimensional plot.

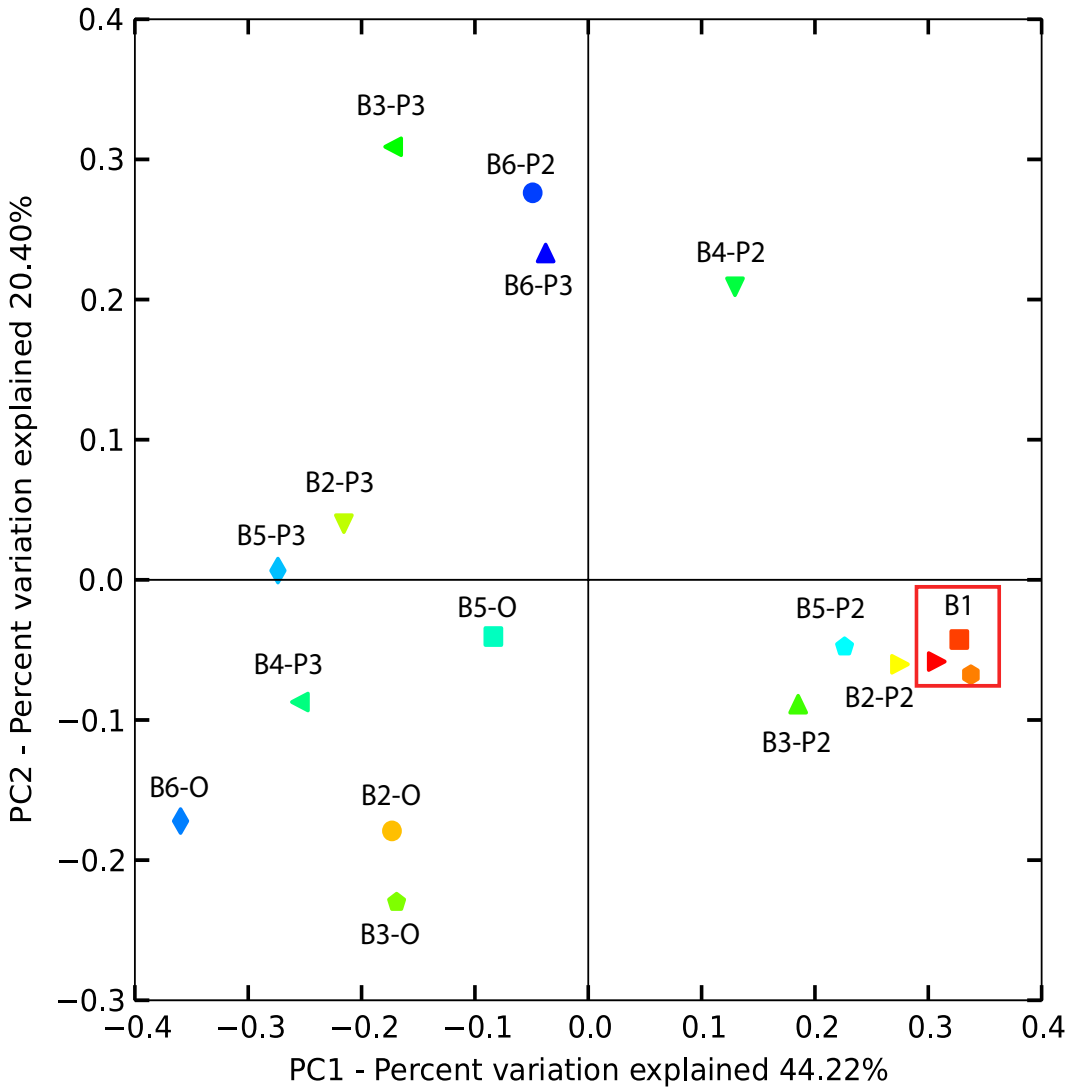

Figure 23 Principal Coordinate Analysis (PCoA) of May 2013 Samples PCoA scatter plot using the first and second eigenvalues as axes. Eigenvalues were calculated from weighted UniFrac distance matrices of each sample data set. B1-B6 corresponds to each Bioreactor while P2-O corresponds to the sampled port.

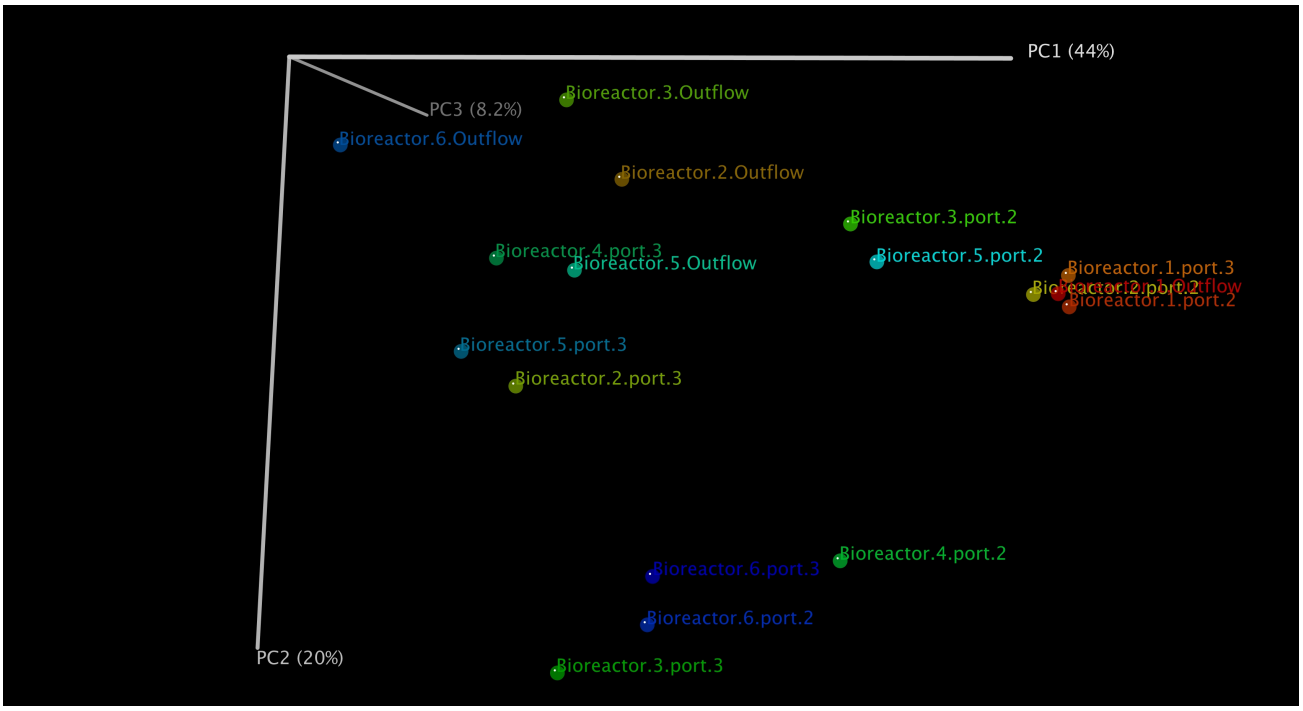

Figure 24 3D PCoA Scatter Plot of May 2013 Samples 3-dimensional scatter plot of PCoA plotted against the first, second, and third eigenvalues. Eigenvalues were calculated from weighted UniFrac distance matrices of each sample set.

Figure 25 shows the UPGMA hierarchical clustering map for the May 2013 sequencing effort. Samples from Bioreactor 1 clustered with high confidence with Port 2 samples from the experimental bioreactors, with the exception of Bioreactor 6. Although the confidence within the groupings is relatively low, the Port 3 and Outflow samples appear to cluster together as well, again with the exception of the Bioreactor 6 Port 2 and 3 samples. The Bioreactor 6 Port 2 and Port 3 samples formed their own cluster with Bioreactor 3 Port 3 at high confidence.

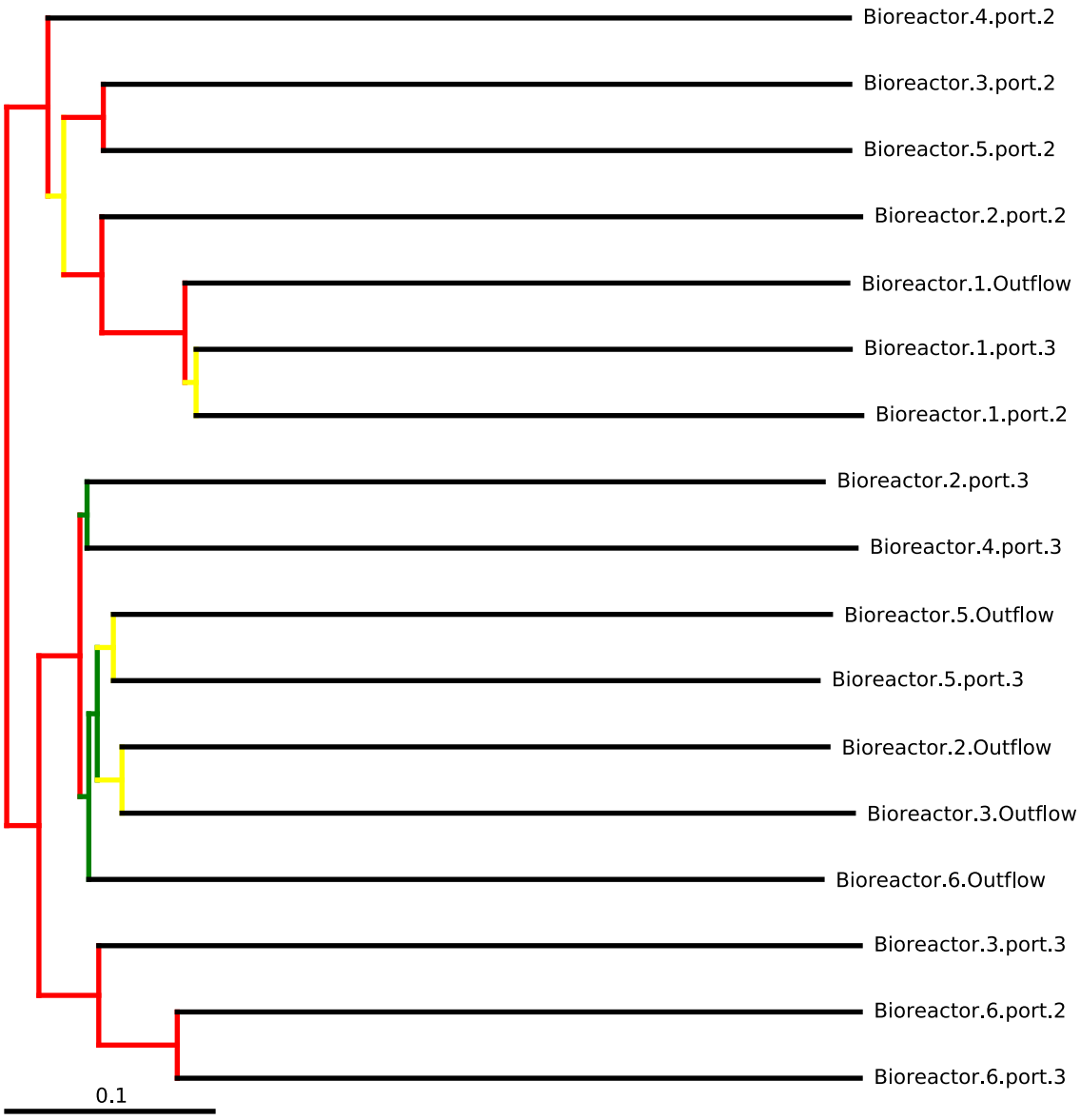

Figure 25 May 2013 UPGMA Hierarchical Cluster Tree Unweighted Pair Group Method with Arithmetic mean hierarchical clustering tree. Tree was constructed using UniFrac distance matrices. Tree node colors indicate jackknife support levels of 75-100% (Red), 50-75% (Yellow) and 25-50% (Green). Scale bar represents branch length changes per distance matrix site.

Statistical Tests

Two multivariate tests of variance were used to determine the effect of both depth and substrate. **Table 4** shows the results of both ANOSIM and adonis methods (Anderson, 2001;

Clarke, 1993; Confais, 1982). The adonis results from the August 2012 samples indicate that 18.56% of the variation between the samples was attributed to the port the sample was taken from (Depth), while 34.92% of the variation is explained by which bioreactor the sample was taken from (Substrate). The ANOSIM test determined that the depth of the sample was not a significant factor to explain the sample variation (*p*-value of 0.07), while the substrate composition of each mixture was a significant factor, although with a calculated R-value of only 0.30.

The adonis test for May 2013 samples showed a decrease in the effect of depth on sample variation to 15.83%. However, an increase to 39.63% of the effect of substrate on the sample variation was seen. ANOSIM results showed more dissimilarity resulted from substrate (0.399 R-value) than depth (0.2547). The R-value for substrate grouping increased by almost 0.1, from August 2012 to May 2013.

Table 4 Statistical tests of variance.

Statistical Test	Df	R Stastic	*p*-value
August 2012 Samples			
adonis			
Depth	2	0.18562	0.009
Substrate	5	0.35921	0.03
ANOSIM			
Depth	N/A	0.2255	0.07
Substrate	N/A	0.3000	0.016
May 2013 Samples			
adonis			
Depth	2	0.1583	0.039
Substrate	5	0.3963	0.003
ANOSIM			
Depth	N/A	0.2547	0.015
Substrate	N/A	0.399	0.009

Df- Degrees of Freedom

R Statistic refers to R^2 for adonis results and R-Value for ANOSIM results

Quantitative Polymerase Chain Reaction

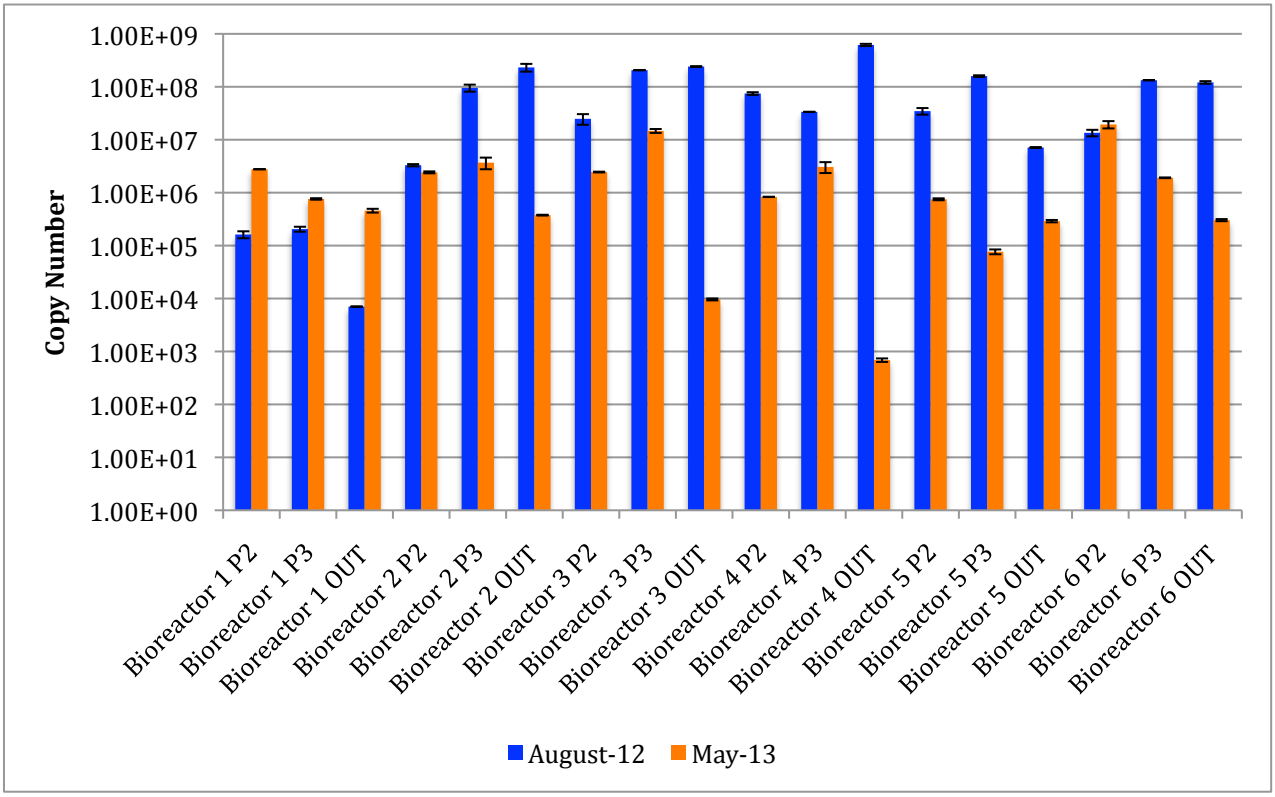

Figure 26 16S rRNA Gene qPCR Estimated gene copy number per 15 ng of DNA extracted from each sampling port from samples taken in August 2012 and May 2013 are shown. All qPCR data consists of triplicate samples, run in at least 2 separate qPCR experiments on separate days with separate reaction constituents.

Gene copy numbers for both 16S rRNA and *dsrB* genes were quantified using quantitative polymerase chain reaction (qPCR). Samples collected from each reactor port in August 2012 and May 2013 were quantified. 15 ng of genomic DNA were used for 16S rRNA gene quantification while 30 ng were used for *dsrB* gene quantification. **Figure 26** shows the estimated 16S rRNA gene copy number from each port and sampling date. In most cases, the 16S rRNA gene copy number decreased during the course of the experiment. The greatest copy number decrease between the two sets of samples was seen from Bioreactor 3 Port 3, with an almost 4-fold decrease between the two sampling points. Samples from Bioreactor 1, the

substrate-lacking control reactor, showed an increase in copy number at all three sampling ports. Bioreactor 6 Port 2 also showed a slight increase in copy number over time, although the change is negligible when the standard deviation of the two samples is considered.

In addition to 16S rRNA gene quantification, the *dsrB* gene was also utilized as a marker for SRB. At the first sampling point (August 2012) the Outflow ports of Bioreactor 3 and 4 showed a significantly higher *dsrB* copy number than the other ports sampled. As seen in **Figure 27**, the estimated copy number of the *dsrB* gene was much lower than estimated 16S gene copy number in most samples. Bioreactor 1 Port 2 and Bioreactor 5 Port had very similar *dsrB* gene copy number for both sampling times. Bioreactor 2 Port 2 and the Outflows of Bioreactor 1 and 6 were the only sample with a higher estimated *dsrB* copy number from the second sampling. All other ports had significantly lower or non-detectable *dsrB* copies from the second sample date.

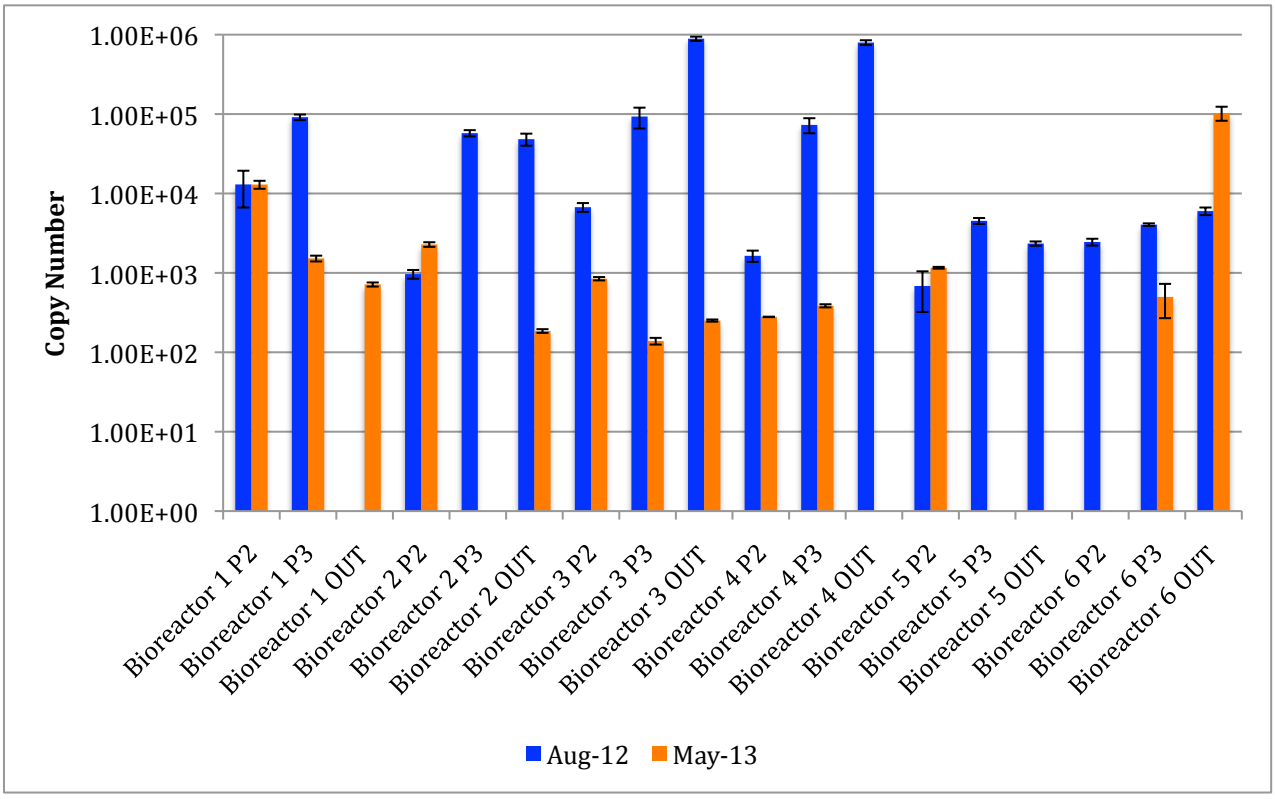

Figure 27 *dsrB* Gene qPCR Estimated gene copy number from each sampling port per 15 ng DNA extracted from samples taken in August 2012 and May 2013 are shown. All qPCR data consists of triplicate samples, run in at least 2 separate qPCR experiments on separate days with separate reaction constituents.

CHAPTER 4

DISCUSSION

Geochemical Data

Geochemical data collected over the course of the study seemed heavily dependent on the seasonal temperature fluctuations of the Southern Illinois. As seen in Figure 3, temperatures varied drastically by season and even within season, ranging from daily averages of below -5˚C to over 28˚C. These fluctuations presumably had an influence on both the abiotic and biotic processes occurring within the bioreactors. While both psychrophilic (e.g. *Desulfofrigus oceanense*) as well as many thermophilic (e.g. *Thermosulfobacterium* species) sulfate-reducing bacteria (SRB) have been cultured and characterized, the majority of cultured SRB have temperature optima between 25˚C and 35˚C (Knoblauch, 1999 and Jeanthon, 2002). Although the temperature of the barrel effluent suggests at least some protection from the most extreme cold temperatures (Fig. 4), it is clear that the SRB community established within the bioreactors was exposed to temperatures well below the normal optimum for the sulfate-reducing community selected for during the first weeks of the study.

This seasonal temperature effect can be seen in the water chemistry data as well. While pH values and sulfate removal percentage in the experimental barrel outflows were initially low (Figs. 5 and 8), each bioreactor saw a steady rise in outflow pH and sulfate-removal percentage until mid-November, the onset of the lowest temperature period faced over the course of the study. Curiously, sulfate removal percentage continually fluctuated as temperatures warmed, but no data collected distinguished any of the substrate ratios (or Bioreactor 1) as being more efficient in sulfate removal.

While Bioreactors 3, 4 and 5 showed a continued decrease in pH after the colder season, Bioreactors 2 and 6 appear to have recovered after ambient temperatures began to rise during early spring (Fig. 5). Bioreactor 1, which lacked a substrate matrix, exhibited an almost immediate decline in pH after exposure to AMD, with outflow pH values rarely reaching more than 1 unit over that of the influent AMD itself. This is most likely a result of reduction in reactive surface area of the limestone without any substrate matrix to mitigate the AMD before it passes through the limestone layer, as is common in constructed passive sulfate-reducing bioreactors (Zagury, 2006 and Johnson 2005).

While the pH of both the AMD stream and Bioreactor 1 remained relatively stable (~2.5-3) throughout the experiment, Figure 6 shows that the influent pH of the experimental barrels ranged drastically over time. While no definite explanation can be provided based on the data collected, several possible factors may have contributed to these results. First, as the reactors with substrate were initially exposed to AMD, the substrate matrix was not yet compacted, resulting in a mixture of substrate in the AMD pool in each reactor. This may have resulted in an environment primed for acidophilic, heterotrophic and photosynthetic organisms (along with abiotic reactions) that contributed to alkalinity generation in the pools, leading to the increase in pH seen. As the bioreactor AMD pools thawed (after December and January freezes), the substrate may have no longer been dissolved in the pools and thus, the microbial communities may have shifted from those capable of substantial alkalinity generation. Another possibility is the effect of seasonal variability on both the metal content and generation rate of AMD. While temperature effects have been discussed already, seasonal variability in rainfall and temperature also contribute to the variability in AMD constituents and thus, the effect of remediation efforts (Kim, 2004 and Edwards, 1999). As rainfall increased and decreased, a two-fold effect may

have been seen in the measured pH of the bioreactor influents. The AMD source itself becomes diluted, with the added water causing a dilution effect on the metal content and pH of the impacted waters (Edwards, 1999). This same dilution effect would also have been seen in the pools themselves, because of their smaller total volume when compared to a full-scale reactor, an influx of water from heavy rainfall might have had a more dramatic impact on measured pH values.

Oxidation-reduction potential (ORP) measurements in experimental bioreactors were also impacted by seasonal changes, although little variation was seen between experimental bioreactor values (Figure 7). Initially, ORP values dropped drastically as microbial communities were established and began the process of metal precipitation. As with pH, ORP increased as temperatures cooled and the bioreactors froze before beginning to decrease as temperatures warmed. ORP values for Bioreactor 1 and the AMD influent increased dramatically as the temperature increased after the winter season, indicating the lack of production of reduced products from the control bioreactor as well as the presence of potential oxidants in influent AMD water. These results are consistent with batch-scale experiments performed *ex situ* (Kijjanapanich, 2012). These results suggest that reduced products (i.e. sulfides) are produced in relatively high amounts due to either biotic or abiotic temperature-sensitive processes. The fact that ORP values were lower in experimental bioreactors during higher-temperature periods of the experiment may indicate a significant contribution of biotic processes to the overall ORP measurements.

Sulfate-Reducing Enrichments

Phylogenetic trees of isolates from sulfate-reducing enrichments were constructed using the Maximum Likelihood (ML) method with a Jukes-Cantor model (Felsenstein, 1985). Two sulfate-reducing bacteria, which appeared closely related to members of the *Desulfovibrio* genus, were isolated using Postgate's Medium C with pyruvate as an electron donor, a medium conducive to sulfate reduction (Fig. 9). *D. desulfuricans* and *D. multispirans* were the closest cultured relatives to each isolate (B3-21 and B3-32), each of which have annotated pathways for sulfate reduction as well as several suspected pathways for pyruvate fermentation (Caspi, 2012). *D. desulfuricans* is also capable of dissimilatory nitrate and nitrite reduction as well as the reduction of several metals including uranium, chromium, mercury and iron (Brown, 2011). While *D. desulfuricans* has been studied extensively, *D. multispirans* has been studied little, known mostly as a close relative of *D. desulfuricans* and *D. gigas*.

In addition to the *Desulfovibrio*-like isolates, three organisms appearing to be related to members of the order *Clostridiales* based on 16S rRNA gene phylogeny were isolated (Fig. 10). Isolate B3-24 was most closely related to *Sporanaerobacter acetigenes,* a strictly anaerobic member of the Cluster XII *Clostridiales* capable of sulfate reduction (Euginio, 2002). *Sporanaerobacter acetigenes* is a moderate thermophile, growing at a temperature range of 25˚C to 50˚C, with an optimum of 40˚C and in a pH range of 5.5-8.5 (Euginio, 2002). *S. acetigenes* is capable of oxidizing a suite of amino acids and sugars along with pyruvate in the presence of sulfate as the terminal electron acceptor (Euginio, 2002).

Isolate B3-35 shared 99% 16S rRNA gene sequence identity with *Clostridium sulfidigenes* and was also very closely related to *Clostridium thiosulfatireducens*. *C.*

thiosulfatireducens is a member of Cluster I of the *Clostridiales* order isolated from several wastewater sites as well as the guts of several animals (Sallam, 2009). This organism is defined by its proteolytic metabolisms (although it can use pyruvate as well), coupling the breakdown of amino acids to the reduction of thiosulfate and elemental sulfur with resultant hydrogen sulfide production (Sallam, 2009).

The final isolate, B3-30, was most closely related to *Clostridium aminobutyricum,* a member of Cluster XI of the *Clostridiales* order (Collins, 1994). *C. aminobutyricum* has been shown to produce hydrogen sulfide from sulfate containing agar slants, to use a suite of amino acids as substrates, and also to reduce nitrate to nitrite (Hardman, 1959). Aside from the initial characterization of the organism and its fermentation of 4-aminobutyrate, little is known about other possible metabolic capabilities (Gerhardt, 2000).

All of the isolated organisms are capable of utilizing sulfur in some oxidized form, be it sulfate, thiosulfate, or elemental sulfur. The closest cultured relatives of SRB-like isolates were members of the *Desulfovibrio* genus capable of both sulfate and nitrate reduction as well as the reduction of metals commonly found in mining pits containing pyrite such as the Tab-Simco mine site. *Clostridiales*-like isolates were also capable of using oxidized sulfur compounds along with a wide array of amino acids and sugars for growth. This is no surprise as the environment they were isolated from initially contained ample supply of whey, a substrate high in the sugar lactose and amino acids. Unfortunately only a partial 16S rRNA segment was used for phylogenetic analysis. For unknown reasons, *E. coli* (Top 10) transformants failed to form colonies after cloning larger PCR fragments (~1500 bps) into pJET and thus could not be used for further analyses. As a result, the phylogenetic identification is limited and some relationships were not fully resolved. It is also unknown why enrichments from Bioreactor 3 showed signs of

growth while others did not. This may have been due to sampling technique (exposure to oxygen) affecting the other enrichment attempts, or it may have been the result of an established community within the sample drawn from Bioreactor 3 that allowed the enrichments to survive transport to the lab and plating more successfully than others.

Fluorescent *in situ* Hybridization (FISH)

Fluorescent probes targeting *Alphaproteobacteria* (ALF968), *Betaproteobacteria* (BET42a), *Deltaproteobacteria* (Delta495a) and *Acidobacteria* (Acido 189) were used to determine the relative abundance of each group in the upper ports (Port 1 and 2) and lower ports (Port 3 and Outflow) of each bioreactor (Fig. 11). The most abundant group of organisms in the upper ports were the *Alphaproteobacteria,* a class which includes members of the *Sulfitobacter, Acidiphilium,* and *Rickettsia* genera along with several phototrophic genera, all of which are commonly found in AMD environments (Baker, 2003 and Williams, 2007). While *Alphaproteobacteria* represented up to 16% of the relative abundance in the upper ports (and Bioreactor 1 samples), they attributed no more than 4% of the total cell abundances of the lower ports. The same can be said of the *Acidobacteria*, which were seen in higher abundance in general in the upper ports than lower ports. The class *Acidobacteria* contains several genera of acidophilic organisms that are prevalent in AMD including *Acidopila, Acidobacterium,* and *Acidicapsa* (Kleinsteuber, 2007). Considering the probable influence of the influent AMD on the communities of the upper ports it is reasonable to assume they would have the highest percentage of cells from the class that contains many common AMD genera. As the AMD

influence is mitigated by the metabolic activity of established bacterial communities in the substrate matrix, the prevalence of those species appears to be reduced.

The *Betaproteobacteria* represented between 4-9% of the relative abundance of each sample, with no apparent discretion between upper and lower ports. Genera of note pertaining to AMD within the *Betaproteobacteria* include *Thiobacter, Thiomonas, Thiobacillus*, *Nitrosomonas*, *Nitrosospira*, and *Ferribacterium* (Garrity, 2007). Members of these genera carry out essential redox reactions within the sulfur, nitrogen and iron cycles in a given environment. While specific genera cannot be counted using the probes in this study, the metabolic diversity within the *Betaproteobacteria* may explain why they are present in similar abundance in both upper and lower ports.

The *Deltaprotobacteria* were the least abundant class of those counted using FISH. The relative abundance appeared to be higher in lower port samples than upper ports. Although not the only members, the most important genera of *Deltaproteobacteria* in AMD sites are the SRB within this class including *Desulfovibrio, Desulfobacula, Desulfomicrobium, Desulfosarcina, Desulfobacterium* and *Desulfobacter* (Castro, 2000 and Plugge, 2011). These organisms are either strict or facultative anaerobes, and thus would occupy niches low in or devoid of oxygen. If most of the detected *Deltaproteobacteria* were SRB, their prevalence would be expected in lower ports where less exposure to atmospheric oxygen occurs due to the AMD pools and substrate matrices within each bioreactor.

When compared to pyrosequencing data from August 2012 (discussed below), relative abundances calculated from FISH data correspond in several situations (Figs. 11 and 12). *Alphaproteobacteria* were more abundant in Port 2 samples and upper samples, although the relative abundance in several of the Port 2 samples was much higher than those detected by

FISH. The *Acidobacteria* abundances in Port 2 of Bioreactor 5 and 6 were similar to those detected in the upper port samples using FISH, although the other FISH abundances appear to be overestimates. *Betaproteobacteria* and *Deltaproteobacteria* appeared overrepresented in the FISH data in all but Bioreactor 1 samples. While it appeared that FISH might be a viable option for cell enumeration from the bioreactors in the future, probes for the current study were chosen prior to the acquisition of pyrosequencing data. As a result, the most numerous classes (*Clostridium* and *Bacillus*) according to the sequence data were not included in the FISH analysis. In future experiments, probes will be used based on the sequence abundance and other factors.

Pyrosequencing Analysis

In order to gain insight into the changes occurring in the bacterial community present within each bioreactor over time, DNAs from samples collected in August 2012 and May 2013 were sequenced using 454 pyrosequencing and analyzed using the QIIME pipeline (Caporoso, 2010). August 2012 samples showed a limited diversity at both the class and genus level (Figures 12-15). Many genera of acid tolerant and acidophilic organisms were represented, including members of the *Alphaproteobacteria* and *Bacilli*. The most abundant sequences belonged to the family *Veillonellaceae,* a family of *Clostridia* which contains the genus *Megasphaera,* a common organism found in ruminant gut samples, which is used as a probiotic treating acidosis in cattle (Aikman, 2011). *M. eldensii* is particularly important because of its metabolic pathways for mitigating the pH drop associated with lactic acid production by lactic acid bacteria (Aikman, 2011), the most prevalent group of *Bacilli* in August 2012 samples. The

prevalence of each of these groups suggests a community similar to that of an acidified bovine rumen, which persisted immediately after the bioreactors were exposed to AMD.

The substrate complexes within each barrel, each containing 17.6 L of bovine manure and 8.8 L of whey, provided ample substrate in the form of lactose to the acid resistant populations present within the manure. As the lactic acid bacteria metabolize the carbohydrates provided in whey, organisms such as *Megasphaera* species can readily metabolize the by products (lactate and acetate) while withstanding the low pH produced by AMD and lactic acid. In addition, the carboxylic acids and other short chain carbon molecules can be used as substrates for other organisms, including SRB (Marx, 2011 and Plugge, 2011). Obviously, a multitude of organisms and metabolic consortia contribute to the establishment of any community. However, based on the abundance of sequences similar to *Megasphaera* and other lactic acid bacteria, they likely played a prominent role in the establishment of the initial microbial community within the bioreactors.

Due to the nature of the substrates selected for the bioreactors coupled with the limited time that passed before the first sampling, little variation was seen based on the substrate ratio. Most likely the nutrients available from the manure and whey, and possibly the spent brewing grains, were sufficient for the early community members. After such a short time it is unlikely that either the simple or complex substrates had been broken down enough to play a substantial role in the metabolic processes occurring. This is evident in the beta-diversity and statistical analyses performed on the August 2012 sequencing data. Principal Coordinate Analysis (PCoA) and Unweighted Pair Group Method with Arithmetic mean (UPGMA) hierarchical clustering showed a distinct grouping between samples based on depth rather than substrate composition. This may again be a function of the AMD permeating into the substrate matrix, affecting the

communities less and less at lower depths. This would explain why Port 2 samples grouped together apart from Port 3 and Outflow samples, which were impacted by AMD conditions less as it flowed through the matrix and was mitigated. It is also likely that Bioreactor 1 samples, which lacked a substrate matrix, grouped together as a result of the bacterial AMD community remaining similar at each depth. Statistical analysis using both adonis and ANOSIM statistical tests indicated that a higher degree of the difference between samples could be attributed to the substrate than the depth (i.e. communities shared less similarity when grouped based on substrate than depth). As expected, the community diversity of the bioreactors from August 2012 samples was relatively low and not dependent on the composition of substrate matrix in each bioreactor.

After ten months (May 2013) of AMD exposure, sample alpha-diversity increased by all measures (Figs. 19-22). Increases in the observed OTUs as well as Faith's phylogenetic diversity were seen in most samples when compared to August 2012. Shannon diversity and chao1 richness estimates were also higher overall in samples with a full compliment of sequences. This indicates that species richness, species diversity, as well as the phylogenetic diversity (as determined by the total branch length of each samples constructed ML trees), increased over the ten-month period. This is also apparent in Figure 21, with a clear increase in the amount and distribution of OTUs that represent at least 0.125% of the total sequences. There was a large increase in the number of OTUs belonging to families and genera of acidophilic organisms commonly found in AMD-like environmental samples. These include members of the *Acidimicrobiaceae*, *Acerobacteraceae*, *Acidithiobacilliaceae*, and *Alicyclobacillaceae* (Kimura, 2011; Schippers, 2010 and Rowe, 2007). Of these families, members of the *Acidothiobacillus* genus are considered the most important in AMD impacted sites (Nancucheo, 2011 and Rowe, 2007). Members of this genus are capable of the oxidation of a variety of reduced inorganic

sulfur compounds (RISCs) and one species (*A. ferrooxidans*) can readily oxidize ferrous iron (Kelly, 2000). *Acidithiobacillus* species have also been shown to utilize oxidized sulfur compounds and ferric iron as terminal electron acceptors under anaerobic conditions (Ohmura, 2002). The drastically increased presence of *Acidithiobacillus* species and other acidophilic chemolithotrophs over the ten-month study illustrates the shift of the microbial community from one dominated by heterotrophic bacteria adapted to life in the acidic bovine rumen to a community more reliant on redox reactions utilizing the metal species present within the AMD entering the bioreactors.

Also of note is the increase in population of bacteria with the potential to degrade plant material (notably cellulose). Large increases in *Bacteroidia* sequences were seen in the lower port (Port 3 and Outflow) samples from May 2013. Members of this class, along with several genera detected (including *Cellulomonas* species), have been studied for their ability to degrade plant cell wall material such as lignin and cellulose through hydrolysis and fermentation (Salyers, 1977). The presence of these organisms, along with members of the *Actinobacteria*, suggests that plant materials had begun to be enzymatically decomposed (Das, 2006). Surprisingly, sequences belonging to possible cellulolytic bacteria were present in high abundances in bioreactors containing both high and low simple:complex substrate ratios. After only ten months it was expected that reactors 3 and 5, which contained the highest ratio of simple to complex substrate (70:30 and 90:10, respectively), would exhibit the largest populations of bacteria that thrive on the fermentation of plant material. However, the possibility that complex substrates (wood chips and saw dust) had also begun to be degraded cannot be discounted. In addition, many *Clostridium* species along with several species of fungi may have contributed to the breakdown of cellulosic substrate (Das, 2006 and Baldy, 1995).

In addition to the increase in chemlithotrophic and cellulolytic populations, the 16S rRNA gene of several genera of sulfate-reducing bacteria was detected at significant levels. Sequences similar to the genera *Desulfurella* and *Desulfosporosinus* and the family *Desulfobacteraceae* were found in both upper and lower port samples in most of the bioreactors. Species of *Desulfurella* are moderately thermophilic and neutrophilic anaerobes that couple the reduction of thiosulfate or elemental sulfur to the oxidation of short chain organic and fatty acids for energy generation (Miroshnichenko, 1998). *Desulfosporosinus* species are mesophilic, acidophilic to neutrophilic, strict anaerobes capable of reducing both sulfate and thiosulfate while oxidizing organic compounds incompletely to acetate (Robertson, 2001). The presence of these organisms, along with the wide array of sulfate-reducing metabolisms exhibited by the *Desulfobacteraceae* are an encouraging sign that conditions within the substrate matrices of the bioreactors are conducive to SRB proliferation. It also appears that, within the sampled areas, niches for the reduction of a variety of sulfur compounds (sulfate, thiosulfate, elemental sulfur) have formed.

Beta diversity metrics and statistical analyses from May 2013 sequences showed a less distinct pattern than August 2012 samples. First, Bioreactor 1 samples seemed to cluster with the Port 2 samples of several bioreactors while the majority of Outflow samples clustered with Port 3 samples. The Outflow and Port 3 samples were widely dispersed throughout the coordinate axes and UPGMA hierarchy (Figs 23-25). The only rough clustering based on substrate occurred between Ports 2 and 3 of Bioreactor 6, which clustered together along with the Bioreactor 3 Port 3 sample. It should be noted here that the lack of defined clustering might be a result of the increased sequence diversity found in May 2013 samples. While August 2012 samples were dominated by a relatively small group of OTUs, the sequence distribution seen in

May 2013 was more diverse. This may have resulted in a larger disparity between the samples based on Unifrac distances and principal coordinates analysis.

ANOSIM and adonis statistical analyses showed a decrease in the effect of sample variation based on depth, and an increase based on differential substrate ratio. These results indicate that as time progressed, the variation between the bacterial communities present within each bioreactor was influenced more by the substrate in each bioreactor than the port from which they were collected. This was true for both sample dates, the variation attributed to substrate only increased as time progressed, while the variation attributed to depth actually decreased according to the adonis test. While it would be beneficial to run statistical analyses based on sample similarity as opposed to sample variation, limitations in the current QIIME pipeline configuration require multivariate data be converted to matrix format for such analyses. Since Unifrac is the only available matrix, and it is a distance-based method, only statistical analyses based on variation were appropriate for the current study (Lozupone, 2007).

Quantitative Polymerase Chain Reaction

Estimates of 16S rRNA gene and *dsrB* gene copy number were carried out using quantitative polymerase chain reaction (qPCR) experiments. Decreases in 16S rRNA gene copy number between August 2012 and May 2013 samples were seen in all samples, excluding samples from Bioreactor 1 and Bioreactor 6 Port 2 (Fig. 26). Initially the bacterial communities were supplied with ample nutrition in the form of whey and manure, along with the varied substrates added to each bioreactor. The bacterial communities present in the manure, already adapted to moderate acidity, were able to proliferate relatively easily during the first

measurement time points. As the experiment progressed, nutrients from the whey and manure may have been exhausted and thus the heterotrophic bacterial community would be reliant on the degradation of plant material in the substrate matrix (or possible photosynthetic processes) for organic carbon and nutrients while the chemolithotrophic community relied on the influx of metal sulfides and iron compounds for use in various redox pathways. This possibility, coupled with the continuous mitigation of low pH conditions, may have resulted in a smaller bacterial community size in May 2013.

The estimated copy number of *dsrB* genes also decreased from August 2012 to May 2013 in all samples excluding Bioreactor 2 Port 2 and Bioreactor 6 Outflow (Fig. 27). This may be indicative of the substrate composition being more effective at SRB stimulation, but further study will be required at several later time points to determine if this is actually the case. The same explanation may be applicable to both the *dsrB* and 16S rRNA data, as the total cell abundance may have been lower due to harsher environmental conditions. There is also the possibility of inhibition due to remaining contaminants in the DNA samples. May 2013 samples were black in color and smelled of sulfide, presumably the result of hydrogen sulfide and metal sulfide compounds. While extraction measures and dilutions were performed in attempt to limit any inhibition, the possibility cannot be ruled out. In addition, the fact that 16S rRNA gene copy number increased in Bioreactor 1 samples (which lacked any obvious sulfide production) may also indicate that precipitates in May 2013 may have had an inhibitory effect on detected copy number in both assays. It should also be noted that in order to estimate the quantity of *dsrB* genes 30 total ng of DNA were required while only 15 ng were required for 16S rRNA gene experiments.

Conclusions

Current data collected from the bioreactors indicate that the most important factors in the remediation of AMD are the seasonal changes experienced by PSRBs. Chemical data suggests that the remediation efficiency of PSRBs is determined by the local weather patterns, more so than the substrate ratio differences within each bioreactor. While SRB were detected in culture and 16S rRNA gene sequences, no distinctions can be made thus far about the effect of substrate ratio on the mitigation of AMD impacted water sources. Community analyses by 16S rRNA gene pyrosequencing suggest a shift in the microbial community within each bioreactor from one dominated by common ruminant bacteria to a more diverse community containing organisms with prevalent roles in the iron, carbon, and sulfur cycles of AMD communities. While community diversity based on substrate composition increased over the course of the study, further analyses are required to determine the long-term role of variation in simple and complex substrates in PSRBs.

REFERENCES

Aikman P. C., P. H. Henning, D. J. Humphries, and C. H. Horn. 2011. Rumen pH and fermentation characteristics in dairy cows supplemented with *Megasphaera elsdenii* NCIMB 41125 in early lactation. Journal of Dairy Science **94**:2840–2849.

Amann R. I., B. J. Binder, R. J. Olson, S. W. Chisholm, R. Devereux, and D. A. Stahl. 1990. Combination of 16S rRNA-targeted oligonucleotide probes with flow cytometry for analyzing mixed microbial populations. Applied and Environmental Microbiology **56**:1919-1925.

Anderson, M.J. 2001. A new method for non-parametric multivariate analysis of variance. Austral Ecology **26**:32-46.

Baker B. J., D. P. Moser, B. J. Macgregor, S. Fishbain, M. Wagner, N. K. Fry, B. Jackson, N. Speolstra, S. Loos, K. Takai, B. S. Lollar, J. Fredrickson, D. Balkwill, T. C. Onstott, C. F. Wimpee, and D. A. Stahl. 2003. Related assemblages of sulphate-reducing bacteria associated with ultradeep gold mines of South Africa and deep basalt aquifers of Washington State. Environmental Microbiology **5**:267–277.

Baker, B. J. and J. F. Banfield. 2003. Microbial communities in acid mine drainage. FEMS Microbiology Ecology. **44**:139-152.

Baldwin D. S., and M. Fraser. 2009. Rehabilitation options for inland waterways impacted by sulfidic sediments--a synthesis. Journal of Environmental Management **91**:311–319.

Baldy V., M. O. Gessner, and E. Chauvet. 1995. Bacteria, Fungi and the breakdown of leaf litter. OIKOS. **74**:94-102.

Behum P. T., L. Lefticariu, K. S. Bender, Y. T. Segid, A. S. Burns, and C. W. Pugh. 2011. Remediation of coal-mine drainage by a sulfate-reducing bioreactor: A case study from the Illinois coal basin, USA. Applied Geochemistry **26**:S162–S166.

Bekmezci O. K., D. Ucar, A. H. Kaksonen, and E. Sahinkaya. 2011. Sulfidogenic biotreatment of synthetic acid mine drainage and sulfide oxidation in anaerobic baffled reactor. Journal of Hazardous Materials **189**:670–676.

Brown S. D., C. C. Gilmour, A. M. Kucken, D. Wall, D. A. Elias, C. C. Brandt, M. Podar, O. Chertkov, B. Held, D. C. Bruce, C. John, R. Tapia, C. S. Han, L. A. Goodwin, J. Cheng, S. Pitluck, T. Woyke, N. N. Ivanova, J. Han, S. Lucas, A. L. Lapidus, M. L. Land, L. J. Hauser, A. V Palumbo, J. D. Wall, J. C. Detter, and N. Mikhailova. 2011. Genome sequence of the mercury-methylating strain *Desulfovibrio desulfuricans* ND132. Journal of Bacteriology. **193**:2078–2080.

Burns A. S., C. W. Pugh, Y. T. Segid, P. T. Behum, L. Lefticariu, and K. S. Bender.

2012. Performance and microbial community dynamics of a sulfate-reducing bioreactor treating coal generated acid mine drainage. Biodegradation **23**:415–429.

Caporaso J. G., J. Kuczynski, J. Stombaugh, K. Bittinger, F. D. Bushman, E. K. Costello, N. Fierer, A. G. Pena, J. K. Goodrich, J. I. Gordon, G. A. Huttley, S. T. Kelley, D. Knights, J. E. Koenig, R. E. Ley, C. A. Lozupone, D. McDonald, B. D. Muegge, M. Pirrung, J. Reeder, J. R. Sevinsky, P. J. Turnbaugh, W. A. Walters, J. Widmann, T. Yatsunenko, J. Zaneveld and R. Knight. 2010. QIIME allows analysis of high-throughput community sequencing data. Nature Methods. **7**:335-336.

Caspi R., H. Foerster, C. a Fulcher, P. Kaipa, M. Krummenacker, M. Latendresse, S. Paley, S. Y. Rhee, A. G. Shearer, C. Tissier, T. C. Walk, P. Zhang, and P. D. Karp. 2008. The MetaCyc Database of metabolic pathways and enzymes and the BioCyc collection of Pathway/Genome Databases. Nucleic acids research **36**:D623–D631.

Castro H. F., N. H. Williams, and A. Ogram. 2000. Phylogeny of sulfate-reducing bacteria **31**:1-9.

Church C. D., R. T. Wilkin, C. N. Alpers, R. O. Rye, and R. B. McCleskey. 2007. Microbial sulfate reduction and metal attenuation in pH 4 acid mine water. Geochemical Transactions **8**:10-24.

Clarke K. R. 1993. Non-parametric multivariate analysis of changes in community structure. Australian Journal of Ecology **18**:117-143.

Collins, M. D., Lawson, P. A., Willems, A., Cordoba, J. J., Fernandez- Garayzabal, J., Garcia, P., Cai, J., Hippe, H. & Farrow, J. A. E. 1994. The phylogeny of the genus *Clostridium*: proposal of five new genera and eleven new species combinations. International Journey of Systematic Bacteriology **44**:812–826.

Colmer, A. R., and M. E. Hinkle. 1947. The role of microorganisms in acid mine drainage: A preliminary report. Science **106**:253-256.

Confais, J., S. Bonnefous, J. Brenot, and J. Pages. 1982. Adonis: A dynamic APL interactive package for multivariate analysis. APL '82 Proceedings of the International Conference on APL. 78-83.

Dahl, C., N. M. Kredich, R. Deutzmann, and H. G. Truper. 1993. Dissimilatory sulphite reductase from *Archaeoglobus fulgidus*: physico-chemical properties of the enzyme and cloning, sequencing, and analysis of the reductase genes. Journal of General Microbiology **139**: 1817–1828.

Das M., T. V Royer, and L. G. Leff. 2007. Diversity of fungi, bacteria, and actinomycetes on leaves decomposing in a stream. Applied and Environmental Microbiology **73**:756–767.

Denef V. J., R. S. Mueller, and J. F. Banfield. 2010. AMD biofilms: using model

communities to study microbial evolution and ecological complexity in nature. The ISME Journal **4**:599–610.

Dopson M., and D. B. Johnson. 2012. Biodiversity, metabolism and applications of acidophilic sulfur-metabolizing microorganisms. Environmental Microbiology **14**:1–12.

Druschel G. K., B. J. Baker, T. M. Gihring, and J. F. Banfield. 2004. Acid mine drainage biogeochemistry at Iron Mountain, California. Geochemical Transactions **5**:13-32.

Edwards K. J., T. M. Gihring, F. Jillian, and J.F. Banfield. 1999. Seasonal variations in microbial populations and environmental conditions in an extreme acid mine drainage environment. Applied and Environmental Microbiology **65**:3627–3632.

Edwards K. J., M. O. Schrenk, R. H. HAmers, and J. F. Banfield. 1998. Microbial oxidation of pyrite: Experiments using microorganisms from an extreme acidic environment. American Mineralogist **83**:1444–1453.

Faith D. P. 1992. Conservation evaluation and phylogenetic diversity. Biological Conservation **61**:1-10

Felsenstein, J. 1985. Phylogenies and the comparative method. The American Naturalist. **125**:1-15

Foti M., D. Y. Sorokin, B. Lomans, M. Mussman, E. E. Zacharova, N. V Pimenov, J. G. Kuenen, and G. Muyzer. 2007. Diversity, activity, and abundance of sulfate-reducing bacteria in saline and hypersaline soda lakes. Applied and Environmental Microbiology **73**:2093–2100.

Fuchs B. M., J. Pernthaler, T. J. Beveridge, A. Breznak, G. Marzluf, T. M. Schmidt, R. Amann, W. Ludwig, M. Wagner, B. Sattler, A. Wille, A. Alfreider, R. Psenner, and K. Trebesius. 2010. Single cell identification by in situ hybridization. Methods for General and Molecular Microbiology **3**:886–896.

Gadd G. M. 2010. Metals, minerals and microbes: geomicrobiology and bioremediation. Microbiology **156**:609–643.

Garrity G. M., T. G. Lilburn, J. R. Cole, S. H. Harrison, J. Euzéby, and B. J. Tindall. 2007. Taxonomic Outline of the Bacteria and Archaea, Release 7 . 7 March 6, 2007 . Part 4 – The Bacteria : Phylum " Proteobacteria ", Class Betaproteobacteria **000012680**:112–147.

Gerhardt A., D. Cinkaya, D. Linder, G. Huisman and W. Buckel. 2000. Fermentation of 4-aminobutyrate by *Clostridium aminobutyricum*: Cloning of two genes involved in the formation and dehydration of 4-hydroxybutyryl-CoA. Archael Microbiology **174**:189-199

Haferburg G., and E. Kothe. 2007. Microbes and metals: interactions in the environment. Journal of Basic Microbiology **47**:453–467.

Hardman, J. K., T. C. Stadtman. 1959. Metabolism of ω-aminobutyric acid by *Clostridium aminobutyricum* nov. sp. Journal of Bacteriology. **4**:544-548

Hernandez-Eugenio G., M. Fardeau, J. Cayol, B. K. C. Patel, P. Thomas, J. Garcia, and B. Ollivier. 2002. *Sporanaerobacter acetigenes* gen. nov., sp. nov., a novel acetogenic, facultatively sulfur-reducing bacterium. International Journal of Systematic and Evolutionary Microbiology **52**:1217–1223.

Hiibel S. R., L. P. Pereyra, L. Y. Inman, A. Tischer, D. J. Reisman, K. F. Reardon, and A. Pruden. 2008. Microbial community analysis of two field-scale sulfate-reducing bioreactors treating mine drainage. Environmental Microbiology **10**:2087-2097.

Jeanthon C., L. Haridon, A. Banta, , A. Reysenbach, and D. Prieur. 2002. *Thermodesulfobacterium hydrogeniphilum* nov ., a thermophilic, chemolithoautotrophic, sulfate-reducing bacterium isolated from a deep-sea hydrothermal vent at Guaymas Basin. International Journal of Systematic and Evolutionary Microbiology **52**:765–772.

Jennings, S. R., D. R. Neuman, and P. S. Blicker. 2008. Acid mine drainage and effects on fish Health and ecology: A review. Reclamation Research Group Publication, Bozeman, MT.

Johnson D. B., and K. B. Hallberg. 2005. Acid mine drainage remediation options: a review. The Science of the Total Environment **338**:3–14.

Johnson D. B., T. Kanao, and S. Hedrich. 2012. Redox transformations of iron at extremely low pH: Fundamental and applied aspects. Frontiers in Microbiology **3**:96.

Johnson D. B., B. Stallwood, S. Kimura, and K. B. Hallberg. 2006. Isolation and characterization of *Acidicaldus organivorus*, gen. nov., sp. nov.: a novel sulfur-oxidizing, ferric iron-reducing thermo-acidophilic heterotrophic Proteobacterium. Archives of Microbiology **185**:212–221.

Kelly, D. P., and A. P. Wood. 2000. Reclassification of some species of *Thiobacillus* to the newly designed genera *Acidithiobacillus* gen. nov., *Halothiobacillus* gen. nov and *Thermithiobacillus* gen. nov. International Journal of Systematic and Evolutionary Microbiology **50**:511-516.

Kijjanapanich P., K. Pakdeerattanamint, P. N. L. Lens, and a P. Annachhatre. 2012. Organic substrates as electron donors in permeable reactive barriers for removal of heavy metals from acid mine drainage. Environmental Technology **33**:2635–2644.

Kim J. J., and S. J. Kim. 2004. Seasonal factors controlling mineral precipitation in the acid mine drainage at Donghae coal mine, Korea. The Science of the Total Environment **325**:181–191.

Kimura S., C. G. Bryan, K. B. Hallberg, and D. B. Johnson. 2011. Biodiversity and geochemistry of an extremely acidic, low-temperature subterranean environment sustained by chemolithotrophy. Environmental Microbiology **13**:2092–2104.

Kleinsteuber S., F. Muller, A. Chatzinotas, K. Wendt-potthoff, and H. Harms. 2007. Diversity and in situ quantification of Acidobacteria subdivision 1 in an acidic mining lake. FEMS microbiology ecology **63**:107–117.

Knoblauch C., K. Sahm, and B. B. Jørgensen. 1999. PsychrophiIic sulfate-reducing bacteria isolated from permanently cold Arctic marine sediments : description of *Desulfofrigus oceanense* gen. nov., sp. nov., *Desulfofrigus fragile* sp. nov., *Desulfofaba gelida* gen. nov., sp. nov., *Desulfotalea arctica* sp. nov. International Journal of Systematic Bacteriology **49**:1631–1643.

Li D., J. O. Sharp, P. E. Saikaly, S. Ali, M. Alidina, M. S. Alarawi, S. Keller, C. Hoppe-Jones, and J. E. Drewes. 2012. Dissolved organic carbon influences microbial community composition and diversity in managed aquifer recharge systems. Applied and Environmental Microbiology **78**:6819–6828.

Lovley D. R., E. E. Roden, E. J. P. Phillips, and J. C. Woodward. 1993. Enzymatic iron and uranium reduction by sulfate-reducing bacteria. Marine Geochemistry **113**:41-53.

Loy A., F. Maixner, M. Wagner, and M. Horn. 2007. probeBase – an online resource for rRNA-targeted oligonucleotide probes: new features 2007. Nucleic Acids Research **35**:D800-D804.

Lozupone C. A., M. Hamady, S. Kelley and R. Knight. 2007. Quantitative and qualitative (beta) diversity measures lead to different insights into factors that structure microbial communities. Applied and Environmental Microbiology. **73**:1576-1585.

Lu S., S. Gischkat, M. Reiche, D. M. Akob, K. B. Hallberg, and K. Küsel. 2010. Ecophysiology of Fe-cycling bacteria in acidic sediments. Applied and Environmental Microbiology **76**:8174–8183.

Macías F., M. A Caraballo, J. M. Nieto, T. S. Rötting, and C. Ayora. 2012. Natural pretreatment and passive remediation of highly polluted acid mine drainage. Journal of Environmental Management **104**:93–100.

Madigan, M. T., J. M. Martinko, P.V. Dunlap, and D.P. Clark. 2009. Brock Biology of Microorganisms. Twelfth Edition. Pearson Benjamin Cummings, New York, NY. 613-651.

Manz W., R. Amann, W. Ludwig, M. Wagner and K. H. Schleifer. 1992. Phylogenetic oligodeoxynucleotide probes for the major subclasses of *Proteobacteria*: problems and solutions. Systematic and Applied Microbiology **15**:593-600.

Marx H., A. B. Graf, N. E. Tatto, G. G. Thallinger, D. Mattanovich, and M. Sauer. 2011. Genome sequence of the ruminal bacterium *Megasphaera elsdenii*. Journal of Bacteriology **193**:5578–5579.

McCarthy, A. J. 1987. Lignocellulose-degrading actinomycetes. FEMS Microbiology Review. **46**:145–163.

Meisinger, D. B., J. Zimmermann, W. Ludwig, K. Schleifer, G. Wanner, M. Scmid, P. C. Bennett, A. S. Engel, and N. M. Lee. 2007. In situ detection of novel *Acidobcateria* in microbial mats from a chemolithoautotrophically based cave ecosystem (Lower Kane Cave, WY, USA). Environmental Microbiology **9**:1523-1534.

Miroshnichenko M. L., F. A. Rainey, H. Hippe, N. A. Chernyh, and U. T. Dsm. 1998. *Desulfurella propionica* sp. nov., new sulfur-respiring thermophilic bacteria from Kamchatka thermal environments. International Journal of Systematic Bacteriology **48**:475–479.

Nancucheo I., and D. B. Johnson. 2011. Significance of microbial communities and interactions in safeguarding reactive mine tailings by ecological engineering. Applied and Environmental Microbiology **77**:8201–8208.

Neculita C. M., and G. J. Zagury. 2008. Biological treatment of highly contaminated acid mine drainage in batch reactors: Long-term treatment and reactive mixture characterization. Journal of Hazardous Materials **157**:358–366.

Neculita C. M., G.-J. Yim, G. Lee, S.-W. Ji, J. W. Jung, H.-S. Park, and H. Song. 2011. Comparative effectiveness of mixed organic substrates to mushroom compost for treatment of mine drainage in passive bioreactors. Chemosphere **83**:76–82.

Neculita C.-M., G. J. Zagury, and B. Bussière. 2007. Passive treatment of acid mine drainage in bioreactors using sulfate-reducing bacteria: critical review and research needs. Journal of Environmental Quality **36**:1–16.

Neef A. 1997. Application of in situ single-cell population analysis for identification of bacteria in complex microbial biocenosis. Doctoral Thesis. Technical University of Munich.

Norlund K. L. I., G. Southam, T. Tyliszczak, Y. Hu, C. Karunakaran, M. Obst, A. P. Hitchcock, and L. A. Warren. 2009. Microbial architecture of environmental sulfur processes: a novel syntrophic sulfur-metabolizing consortia. Environmental Science & Technology **43**:8781–8786.

Ohmura N., K. Sasaki, N. Matsumoto, and H. Saiki. 2002. Anaerobic respiration using Fe^{3+}, S^0, and H_2 in the chemolithoautotrophic bacterium *Acidithiobacillus ferrooxidans*. Journal of Bacteriology. **184**:2081-2087.

Oren A. 2010. Acidophiles. Encyclopedia of Life Sciences 1–14.

Plugge C. M., W. Zhang, J. C. M. Scholten, and A. J. M. Stams. 2011. Metabolic flexibility of sulfate-reducing bacteria. Frontiers in Microbiology **2**:1–8.

Postgate J. R. 1984. The Sulphate-Reducing Bacteria**,** Second Edition. Cambridge: Cambridge University Press.

Postgate J. R., H. M. Kent, R. L. Robson, and J. A. Chesshyre. 1984. The genomes of *Desulfovibvio gigas* and *D. vulgaris*. Journal of General Microbiology **130**:1597–1601.

Pugh, C. W., P.T. Behum, L. Lefticariu, A.S. Burns, K.S. Bender. 2012. Community Analysis of a Sulfate-Reducing Bioreactor Treating Coal Generated Acid-Mine Drainage. Presented at the American Society for Microbiology, 112th General Meeting, San Francisco, CA. (International).

Rambaut, A. 1996. Se-Al: Sequence Alignment Editor ver. 2.0. [Online]. Program distributed by the author. Department of Zoology, University of Oxford, Oxford. Available: http://tree.bio.ed.ac.uk/software/seal/.

Robertson W. J., J. P. Bowman, P. D. Franzmann, and B. J. Mee. 2001. *Desulfosporosinus meridiei* sp. nov., a spore-forming sulfate-reducing bacterium isolated from gasolene-contaminated groundwater. International Journal of Systematic and Evolutionary Microbiology **51**:133–140.

Rowe O. F., J. Sánchez-España, K. B. Hallberg, and D. B. Johnson. 2007. Microbial communities and geochemical dynamics in an extremely acidic, metal-rich stream at an abandoned sulfide mine (Huelva, Spain) underpinned by two functional primary production systems. Environmental Microbiology **9**:1761–1771.

Salyers A. A., J. R. Vercellotti, S. E. West, T. D. Wilkins. 1977. Fermentation of mucin and plant polysaccharides by strains of *Bacteroides* from the human colon. Applied and Environmental Microbiology. **33**:319–322

Sawicka J. E., B. B. Jørgensen, and V. Brüchert. 2012. Temperature characteristics of bacterial sulfate reduction in continental shelf and slope sediments. Biogeosciences **9**:3425–3435.

Sallam A., and A. Steinbüchel. 2009. Clostridium sulfidigenes sp. nov., a mesophilic, proteolytic, thiosulfate- and sulfur-reducing bacterium isolated from pond sediment. International Journal of Systematic and Evolutionary Microbiology **59**:1661–1665.

Sánchez España J., E. López Pamo, E. Santofimia, O. Aduvire, J. Reyes, and D. Barettino. 2005. Acid mine drainage in the Iberian Pyrite Belt (Odiel river watershed, Huelva, SW Spain): Geochemistry, mineralogy and environmental implications. Applied Geochemistry **20**:1320–1356.

Sánchez-Andrea I., K. Knittel, R. Amann, R. Amils, and J. L. Sanz. 2012. Quantification of Tinto River sediment microbial communities: importance of sulfate-reducing bacteria and their role in attenuating acid mine drainage. Applied and Environmental Microbiology **78**:4638–4645.

Sánchez-Andrea I., N. Rodríguez, R. Amils, and J. L. Sanz. 2011. Microbial diversity in anaerobic sediments at Rio Tinto, a naturally acidic environment with a high heavy metal content. Applied and Environmental Microbiology **77**:6085–6093.

Schippers A., Breuker, A. Blazejak, K. Bosecker, D. Kock, and T. L. Wright. 2010. The biogeochemistry and microbiology of sulfidic mine waste and bioleaching dumps and heaps, and novel Fe(II)-oxidizing bacteria. Hydrometallurgy **104**:342–350.

Singer P. C., and W. Stumm. 1970. Acidic mine drainage: The rate-determining step. Science **167:**1121-1123.

Song H., G.-J. Yim, S.-W. Ji, C. M. Neculita, and T. Hwang. 2012. Pilot-scale passive bioreactors for the treatment of acid mine drainage: Efficiency of mushroom compost vs. mixed substrates for metal removal. Journal of Environmental Management **111**:150–158.

Tamura, K., D. Peterson, N. Peterson, G. Stecher, M. Nei and S. Kumar. 2011. MEGA 5: Molecular evolutionary genetics and analysis using maximum likelihood, evolutionary distance, and maximum parsimony methods. Molecular Biology and Evolution **28**:2731-2739.

Wallner G., R. Amann, and W. Beisker. 1993. Optimizing fluorescent in situ hybridization with rRNA-targeted oligonucleotide probes for flow cytometric identification of microorganisms. Cytometry **14**:136-143.

Wagner, M., A. G. Roger, G. A. Flax, G. A. Brusseau, and D. A. Stahl. 1998. Phylogeny of dissimilatory sulfite reductases supports an early origin of sulfate respiration. Journal of Bacteriology **180**: 2975–2982.

Wagner M. 2002. Oligonucleotide microarray for 16S rRNA gene-based detection of all recognized lineages of sulfate-reducing prokaryotes in the environment. Applied and Environmental Microbioliogy **68**:5064-54

Williams K. P., B. W. Sobral, and A. W. Dickerman. 2007. A robust species tree for the *Alphaproteobacteria*. Journal of bacteriology **189**:4578–4586.

Zagury G. J., V. I. Kulnieks, and C. M. Neculita. 2006. Characterization and reactivity assessment of organic substrates for sulphate-reducing bacteria in acid mine drainage treatment. Chemosphere **64**:944–954.

APPENDICES

APPENDIX A

Fluorescent in situ hybridization raw data

All numbers that were used to calculate the relative cell abundance for each probe and sample port are shown. All lower ports were analyzed with 5 ml of filtrate while all upper ports required 10 ml filtrate. Probe/DAPI percents were corrected by subtracting the Non/DAPI count percentage of each filter.

Table 5 FISH Counts for Bioreactor 1 Ports

Probe	Std Dev (%)	# of Grids	Probe/DAPI (%)
BET42a	3.0	24	4.2
Delta495a	0.7	24	1.4
ALF968	3.7	24	9.5
Acido 189	1.7	24	1.8

Table 6 FISH Counts for Bioreactor 2 Lower Ports

Probe	Std Dev	# of Grids	Probe/DAPI (%)
BET42a	1.5	24	5.5
Delta495a	0.9	24	3.2
ALF968	0.8	24	2.5
Acido 189	1.2	24	2.6

Table 7 FISH Counts for Bioreactor 2 Upper Ports

Probe	Std Dev	# of Grids	Probe/DAPI (%)
BET42a	1.8	24	7.9
Delta495a	0.9	24	2.7
ALF968	NA	NA	NA
Acido 189	NA	NA	NA

Table 8 FISH Counts for Bioreactor 3 Lower Ports

Probe	Std Dev	# of Grids	Probe/DAPI (%)
BET42a	1.4	24	5.0
Delta495a	0.8	24	2.7
ALF968	0.7	24	2.1
Acido 189	1.2	24	2.1

Table 9 FISH Counts for Bioreactor 3 Upper Ports

Probe	Std Dev	# of Grids	Probe/DAPI (%)
BET42a	0.7	24	7.1
Delta495a	0.1	24	1.1
ALF968	2.8	24	12.9
Acido 189	0.7	24	2.6

Table 10 FISH Counts for Bioreactor 4 Lower Ports

Probe	Std Dev	# of Grids	Probe/DAPI (%)
BET42a	1.2	24	7.2
Delta495a	0.7	24	2.9
ALF968	0.6	24	3.4
Acido 189	1.0	24	1.0

Table 11 FISH Counts for Bioreactor 4 Upper Ports

Probe	Std Dev	# of Grids	Probe/DAPI (%)
BET42a	2.3	24	8.8
Delta495a	0	24	0
ALF968	3.0	24	14.2
Acido 189	1.8	24	6.0

Table 12 FISH Counts for Bioreactor 5 Lower Ports

Probe	Std Dev	# of Grids	Probe/DAPI (%)
BET42a	2.8	24	7.5
Delta495a	0.9	24	4.7
ALF968	0.1	24	4.0
Acido 189	0.9	24	1.4

Table 13 FISH Counts for Bioreactor 5 Upper Ports

Probe	Std Dev	# of Grids	Probe/DAPI (%)
BET42a	1.1	24	1.4
Delta495a	0	24	0
ALF968	2.3	24	16.1
Acido 189	0.4	24	7.4

Table 14 FISH Counts for Bioreactor 6 Lower Ports

Probe	Std Dev	# of Grids	Probe/DAPI (%)
BET42a	1.9	24	8.0
Delta495a	0.9	24	3.9
ALF968	0.8	24	2.6
Acido 189	1.3	24	1.3

Table 15 FISH Counts for Bioreactor 6 Upper Ports

Probe	Std Dev	# of Grids	Probe/DAPI (%)
BET42a	2.7	24	8.7
Delta495a	0	24	0
ALF968	2.5	24	15.3
Acido 189	1.7	24	6.5

APPENDIX B

Fluorescent in situ hybridization statistics

Statistical analysis for significant differences between upper and lower port fluorescent in situ hybridization data are shown. The F- and Stident's T- test were used to determine where significant differences lie between the upper ad lower port samples of each bioreactor. (< means relative abundance in upper sample significantly smaller than lower sample, > means relative abundance in the upper sample significantly larger than lower sample, = means no significant difference).

Table 16 FISH Statistical Analysis

Probe	Bioreactor 2	Bioreactor 3	Bioreactor 4	Bioreactor 5	Bioreactor 6
Bet42a	>	>	>	<	=
Delta495a	=	<	<	<	<
ALF968	NA	>	>	>	>
Acido 189	NA	=	>	>	>

VITA

Graduate School
Southern Illinois University

Charles Wayne Pugh

cpugh13@gmail.com

Southern Illinois University-Carbondale
Bachelor of Science, Microbiology, May 2010

Thesis Title: EFFECT OF SUBSTRATE COMPOSITION ON MICROBIAL DIVERSITY AND EFFICIENCY OF *in situ* PILOT-SCALE PASSIVE SULFATE-REDUCING BIOREACTORS TREATING ACID MINE DRAINAGE

Major Professor: Kelly S. Bender

Publications:

Burns, A. S., C. W. Pugh, Y. T. Segid, P. T. Behum, L. Lefticariu, and K. S. Bender. 2011. Performance and microbial community dynamics of a sulfate-reducing bioreactor treating coal generated acid mine drainage. Biodegradation.

Behum, P. T., L. Lefticariu, K. S. Bender, Y. T. Segid, A. S. Burns, and C. W. Pugh. 2011. Remediation of coal-mine drainage by a sulfate-reducing bioreactor: a case study from the Illinois coal basin, USA. Appl Geochem 26:S162-S166.

Presentations:

Pugh, C. W., P.T. Behum, L. Lefticariu, A.S. Burns, K.S. Bender. (2012) "Community Analysis of a Sulfate-Reducing Bioreactor Treating Coal Generated Acid-Mine Drainage". American Society for Microbiology, 112th General Meeting, San Francisco, CA. (International)

Pugh, C. W., Y. T. Segid, P. T. Behum, L. Lefticariu, A. S. Burns, and K. S. Bender. (2010) "Community Analysis of the Acid Mine Drainage from an Abandoned Tab Simco Coal Mine". St. Louis Area Undergraduate Research Symposium, Carbondale, IL (Regional)